Lower Miocene (upper Burdigalian, Karpatian) volcanic ash-fall at the south-eastern margin of the Bohemian Massif in Austria – New evidence from $^{40}Ar/^{39}Ar$-dating, palaeomagnetic, geochemical and mineralogical investigations

Reinhard ROETZEL[1)*], Arjan de LEEUW[2)], Oleg MANDIC[3)], Emő MÁRTON[4)], Slavomír NEHYBA[5)], Klaudia F. KUIPER[6)], Robert SCHOLGER[7)] & Ingeborg WIMMER-FREY[1)]

[1)] Geological Survey, Neulinggasse 38, 1030 Wien, Austria;

[2)] CASP, West Building, 181A Huntingdon Road, Cambridge, CB3 0DH, United Kingdom;

[3)] Department of Geology and Palaeontology, Natural History Museum Vienna, Burgring 7, 1014 Wien, Austria;

[4)] Palaeomagnetic Laboratory, Geological and Geophysical Institute of Hungary, Columbus 17-23, 1145 Budapest, Hungary;

[5)] Institute of Geological Sciences, Faculty of Science, Masaryk University, Kotlářská 2, 611 37 Brno, Czech Republic;

[6)] Faculty of Earth and Life Sciences, Vrije Universiteit Amsterdam, De Boelelaan 1085, 1081 HV Amsterdam, The Netherlands;

[7)] Department of Applied Geological Sciences and Geophysics, University of Leoben, Peter-Tunner-Straße 25, 8700 Leoben, Austria;

[*)] Corresponding author, reinhard.roetzel@geologie.ac.at

KEYWORDS

$^{40}Ar/^{39}Ar$ - geochronology
magnetostratigraphy
zircon studies
geochemistry
Burdigalian
Karpatian
Straning

Abstract

An Early Miocene acidic tuff that accumulated in a small tectonic graben at the south-eastern margin of the Bohemian Massif in north-eastern Austria was dated by means of $^{40}Ar/^{39}Ar$ dating. Feldspar crystals from the tuff have an inverse isochron age of 17.23 ± 0.18 Ma, which is interpreted to reflect its crystallisation age. The tuff shows a reversed palaeomagnetic polarity and can be correlated with chron C5Cr of the late Burdigalian (early Karpatian) and with the lowstand systems tract (LST) of the Bur 4 global 3rd order sea level cycle. The tephra originates from acid (rhyodacitic to dacitic) calc-alkaline arc volcanism. Our study demonstrates that the investigated volcaniclastics are significantly different from other Burdigalian (Eggenburgian, Ottnangian) and Langhian (early Badenian) tephra from the area with regard to their volcanic zircon and Rare Earth element (REE) composition. The volcanic source of the Straning tuffs might be traced back to the western Inner Carpathian volcanic arc. The tuffs are most likely genetically related to the Middle Rhyolite Tuff (late Burdigalian, Karpatian) of northern Hungary and southern Slovakia.

Ein untermiozäner Tuff, der in einem kleinen tektonischen Graben am Südostrand der Böhmischen Masse im Nordosten Österreichs abgelagert wurde, besitzt ein $^{40}Ar/^{39}Ar$-Alter von 17.23 ± 0.18 Ma und zeigt eine reverse paläomagnetische Polarität. Er kann damit mit dem reversen Chron C5Cr des späten Burdigalium (frühes Karpatium) und dem lowstand systems tract (LST) des globalen Meeresspiegel-Zyklus 3. Ordnung Bur 4 korreliert werden. Die Aschen stammen von einem sauren (rhyodazitischen bis dazitischen) kalkalkalischen Vulkanismus eines Inselbogens. Die untersuchten vulkanischen Zirkone und die Verteilung der Seltene Erde Elemente (SEE) zeigen deutliche Unterschiede zu anderen Aschen aus dem Burdigalium (Eggenburgium, Ottnangium) und Langhium (frühes Badenium) dieser Region. Die Aschen können wahrscheinlich auf das Gebiet des westlichen inner-karpatischen vulkanischen Bogens zurückgeführt werden. Sie sind vermutlich mit dem Mittleren Rhyolithtuff aus dem späten Burdigalium (Karpatium) in Nordungarn bzw. der südlichen Slowakei genetisch verwandt.

1. Introduction

Tephra layers are frequently used for correlation and radioisotopic dating of sedimentary packages (e.g., Handler et al., 2006; Wijbrans et al., 2007; Palfy et al., 2007; Abdul Aziz et al., 2010; De Leeuw et al., 2011, 2012; Mandic et al., 2011, 2012). They can provide important marker beds in regional stratigraphy and allow precise correlation across large distances. Moreover, their geochemical composition reflects the geodynamic setting of the volcanism and may help to locate the corresponding volcanic eruption (Šegvić et al., 2014).

The Lower Miocene marine sediments at the south-eastern margin of the Bohemian Massif in the Czech Republic and in Austria are intercalated with several tuffs and tuffite layers described from outcrops (Čtyroký, 1982, 1991; Čižek et al., 1990; Nehyba, 1997; Adamová and Nehyba, 1998; Nehyba and Roetzel, 1999; Nehyba et al., 1999) and drill cores (Roetzel et al., 1994, 2008; Schubert et al., 1999). These intercalations are interpreted as products of distal tephra fallout, and have been subject to various post-depositional alteration processes. Most commonly they are deeply weathered and transformed to bentonites or montmorillonitic clays.

This paper provides granulometric, mineralogical, geochemical, tephrostratigraphic, geochronologic, palaeomagnetic, and zircon typology results for some volcaniclastic tuffs from Straning. These tuffs have previously been $^{40}Ar/^{39}Ar$ dated to 16.6 ± 1.0 Ma by S. Scharbert (in Roetzel et al., 1999b), allowing their rough correlation with the late Burdigalian to Langhian (Karpatian – Badenian). We now present a more precise numerical age estimation by integration of results from $^{40}Ar/^{39}Ar$-geochronological and magnetostratigraphic analyses. New mineralogical and geochemical analyses of bulk rock samples and volcanic glasses also provide valuable information about the nature and location of the tuffs' parental volcanism.

2. Geological setting and outcrop description

The study area is located at the south-eastern margin of the Bohemian Massif in north-eastern Austria. Comprehensive data on its regional geological setting can be found in Roetzel (1994, 1996) and Roetzel et al. (1998) (Fig. 1).

The Straning outcrop is located near the prominent Diendorf fault zone, which is formed by NE-SW oriented sub-parallel dislocations with a sinistral strike-slip character (Roetzel, 1996). This fault zone forms the border between the crystalline upland of the Bohemian Massif and the Miocene sedimentary deposits of the Alpine-Carpathian Foredeep. The morphological slope consists of several steep scarps, numerous spurs and frequent inselberg-like bedrock elevations scattered across the foreland (Roštínský and Roetzel, 2005). Close to the main faults, both the crystalline rocks and the bordering Miocene sediments of the foredeep are heavily sheared and often deeply weathered.

The crystalline rocks of the Bohemian Massif exposed in the direct surrounding of Straning are mostly Precambrian granites of the Thaya-Batholith (Thaya granite). They are overlain by lower Burdigalian (upper Eggenburgian) marine nearshore sediments (Roetzel et al., 1999a) mainly represented by medium to coarse sands and gravel of the Burgschleinitz Formation and in a few exceptional cases also by fine sands of the Gauderndorf Formation. These sediments are disconformably overlain by sandy, shallow marine limestones of the Zogelsdorf Formation (middle Burdigalian, uppermost Eggenburgian - Ottnangian), which laterally and vertically pass into deep-water pelitic sediments of the middle Burdigalian (Ottnangian) Zellerndorf Formation. Drill holes in this area show about 25 - 100 m thick pelites above the Zogelsdorf Formation (Raschka, 1912; Schaffer and Grill, 1951; Roetzel, 1994, 1996).

Diatomites of the Limberg Member, close to the villages Limberg, Oberdürnbach and Parisdorf, are intercalated into clays of the uppermost part of the Zellerndorf Formation (Roetzel, 1996; Roetzel et al., 1999c). Towards the east, the diatomites laterally thin out and are interbedded with the middle Burdigalian (Ottnangian) pelites (Roetzel et al., 2006; Grunert et al., 2010). High portions of smectite in the clays of the Zellerndorf Formation and in volcaniclastic layers of contemporaneous strata as well as the occurrence of quartz, glass and zircons of volcanic origin indicate prominent acidic volcanic input at this time (Roetzel et al., 1994, 2006).

The investigated outcrop is situated in a railway-cut of the Franz-Josefs-Bahn, about 650 m east of Etzmannsdorf and 1 km NNW of Straning (15° 51' 34,2'' E, 48° 37' 09,0'' N, rail kilometres 73.925 – 73.93) (cf. Fig. 1). West of the railway track, a 50 m long and 10 to 14 m wide graben incised into granites of the Thaya-Batholith is filled with Lower Miocene pelitic sediments and volcaniclastics. This graben runs subparallel to the sinistral NE-SW striking Diendorf fault system, marked by several NE-striking sinistral slickensides on the granite walls (Decker in Roetzel et al., 1999b). The surface of the granite shows typical corestone-weathering and limonitic crusts (tafoni-weathering). The main part of the sediment fill is

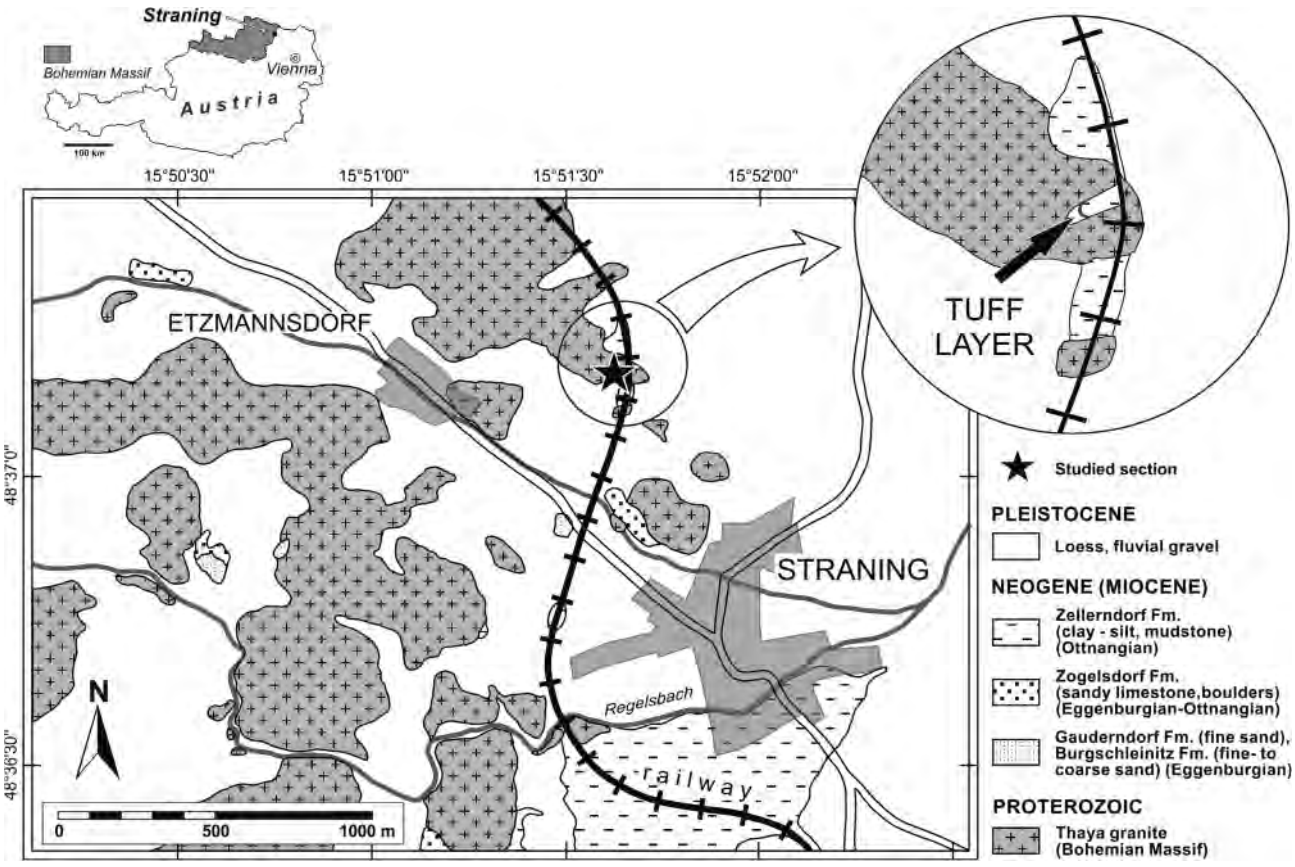

Figure 1: Sketch of the geological situation of the surroundings of the Straning outcrop (map adapted from Roetzel et al., 1998).

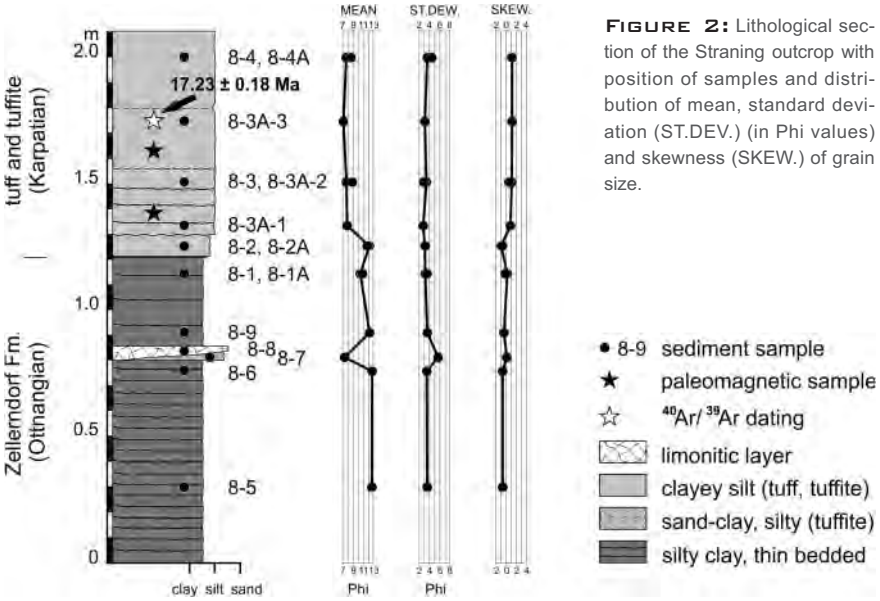

Figure 2: Lithological section of the Straning outcrop with position of samples and distribution of mean, standard deviation (ST.DEV.) (in Phi values) and skewness (SKEW.) of grain size.

affected by a landslide. The fault scarp of the landslide exposes the tuffs and tuffites that are present in the upper part of the sediment fill (cf. Figs. 1, 2, 3). The sediments are slightly tilted to E – SE (090/28 to 120/20) due to the landslide.

The 2.1 m high outcrop (cf. Figs. 2, 3) begins at the base with about 0.8 m greenish-grey, thin and plane bedded silty clays (samples 8-5, 8-6), which are overlain by a 4 to 6 cm thick limonitic layer (sample 8-8). In some parts below this layer relicts of whitish-grey tuffites already occur (sample 8-7). Whitish millimetres thick layers are also recognizable in the 35 cm thick and rather massive pelitic sediments (siltclay; samples 8-9, 8-1, 8-1A) that follow above. Volcanic glass shards already occur in these layers that contain an almost monospecific microfauna consisting of ?*Silicoplacentina* sp. ("*Saccamina*"), with very rare *Triloculina* sp. and fish-teeth (det. I. Cicha). All the clayey sediments at the base of the Straning outcrop are part of the middle Burdigalian (Ottnangian) Zellerndorf Formation.

Seven to ten centimetres of whitish to yellowish grey, soapy silty clays (samples 8-2, 8-2A) follow above a millimetre thick dark-brown clayey layer. The upper part of the outcrop is made up of about 80 cm whitish-grey, indistinctly bedded tuffs and tuffites (claysilt, clayey silt, clayey sandy silt, samples 8-3A-1, 8-3, 8-3A-2, 8-3A-3, 8-4, 8-4A). These volcaniclastics are divided into several cm to dm thick beds interrupted by thin ochre-coloured pelitic layers (cf. Figs. 2, 3).

Figure 3: Outcrop Straning with contact of Zellerndorf Formation (dark base) and upper Burdigalian (lower Karpatian) tuffs and tuffites (light top). Note position of palaeomagnetic samples (drill holes) and of sample for $^{40}Ar/^{39}Ar$ dating (asterisk). Lens cap for scale.

3. Methods

3.1 Granulometry and mineralogy

Thirteen samples for representative grain size analysis were taken (cf. Fig. 2, Tab. 1). Grain size analyses were carried out at the Austrian Geological Survey using a combination of wet sieving in ½ Phi steps and Sedigraph for grain sizes < 0.032 mm. The sieve analysis data and the data generated from the Micromeritics SediGraph 5100 were subsequently calculated and displayed with the software program SedPakWin (Reitner et al., 2005).

The bulk rock and clay mineralogy of five samples (cf. Tab. 2) was determined by XRD at the Department of Mineral Resources of the Austrian Geological Survey. Samples for bulk mineral analysis were dried, ground and loaded into a sample holder as a randomly oriented powder. Diffraction data were collected with a Philips X'Pert Multi Purpose Diffractometer (goniometer PW 3050, CuKα radiation (40 kV, 40 mA), automatic divergence slit, 0.30 mm receiving slit, step size 0.02 °2Θ, 1s/step). The samples were run from 2 – 65 °2Θ. The semiquantitative mineralogical composition was obtained by the SEIFERT AutoQuan software using the Rietveld method.

Samples for clay mineral analysis were treated with 15% H_2O_2 for 24h in order to remove organic matter and subjected to ultrasound for further disaggregation. The <2 µm fractions were separated by centrifugation. The clay fractions were saturated with 1N KCl and $MgCl_2$ solutions by shaking for 24h, and thereafter washed in distilled water. Oriented mounts of the <2µm fractions were made through the suction of 25 mg of suspended clay placed on a porous ceramic plate and left to dry at room temperature. Such oriented XRD mounts were subsequently analysed in air-dried, ethylene glycol, dimethylesulfoxide and glycerol treated states. The clay samples were run from 2 – 50 °2Θ using the same measurement setup, as in the case of bulk-rock samples. Identification of clay minerals was carried out according to Moore and Reynolds (1997). The clay minerals were identified by their basal (00*l*) diffraction lines on glycolated specimens of the Mg-treated samples. The relative percentages of the clay minerals in the fraction < 2 µm were determined after Schultz (1964).

sample		nomenclature	sand (weight %)			silt (weight %)			clay (weight %)	mean (Phi)	stdew (Phi)	skew
			coarse	medium	fine	coarse	medium	fine				
8-4A	top	claysilt	0.02	0.17	7.2	20.4	25.0	18.7	28.6	8.55	4.45	1.05
8-4		clayey silt	0.04	0.18	6.7	19.6	30.9	18.4	24.2	7.86	3.56	1.17
8-3A-3		clayey sandy silt	0.20	0.38	9.7	23.4	31.7	15.6	19.0	7.11	3.04	1.19
8-3A-2		claysilt	0.03	0.07	2.4	6.3	25.8	28.1	37.3	8.83	2.93	0.60
8-3		clayey silt	0.0	0.01	8.3	17.6	30.7	20.6	22.8	7.79	3.37	1.12
8-3A-1		claysilt	0.01	0.05	0.9	20.1	27.7	25.9	25.3	7.90	2.80	0.97
8-2A		silty clay	0.1	0.2	1.4	2.0	4.5	11.9	80.0	11.78	3.13	-0.71
8-2		silty clay	0.05	0.31	0.95	2.6	3.4	8.7	84.0	12.10	3.06	-0.95
8-1A		siltclay	0.2	0.55	0.54	1.3	14.6	21.8	61.1	10.86	3.58	-0.03
8-1		siltclay	0.03	0.10	0.10	1.8	17.4	25.0	55.6	10.31	3.20	0.25
8-9		siltclay	0.09	0.14	0.09	0.9	8.3	17.1	73.4	12.17	3.61	-0.35
8-6		silty clay	0.09	0.12	0.10	0.9	4.5	13.3	81.0	12.79	3.40	-0.65
8-5	base	silty clay	0.04	0.13	0.15	1.4	5.4	13.6	79.3	12.71	3.49	-0.65

Table 1: Grain size distribution of sediments from the Straning outcrop. Nomenclature after Füchtbauer (1959) and Müller (1961). stdew: standard deviation, skew: skewness.

Additionally, the SEM-studies were performed on three samples (sample 8-2, 8-2A, 8-3A-3) using a Tescan Vega 2 XL scanning electron microscope (working parameters 10 kV, 10 mm working distance) at the Austrian Geological Survey (cf. Fig. 5). The mineral phases were analysed by an Oxford Instruments INCA 4.15 energy-dispersive X-ray spectroscopy (EDS).

3.2 Tephrostratigraphy

Zircons from the Straning tuffs were studied in the grain size fraction between 63 and 125 µm. The outer morphology as well as the presence of zonality, cores, and inclusions were studied in the complete zircon population (i.e. volcanic and nonvolcanic/detritic zircons). Typology and elongation studies were only performed for volcanic zircons. Zircon typology (Pupin, 1980) examines the presence or absence of certain crystal planes and interprets the conditions of zircon crystallisation (chemistry and temperature of parental magma). The study of elongation (the relation of length to width of the crystal) is used for tracing the provenance and supporting the volcanic origin of some minerals.

The major elements of volcanic glasses from four samples (samples 8-3A-1, 8-3A-2, 8-4A, and 8-7) were analysed with a CamScan electron microprobe with analyser EDX AN10000 (acceleration voltage 15kV, spot size 72, beam current 2 nA, counting time 60s, well defined homogenous natural and synthetic phases were used as standards, PaP corrections (Pouchou and Pichoir, 1985) in the laboratory of the Faculty of Science, Masaryk University, Brno, Czech Republic (Tab. 3a).

Bulk rock geochemical analyses were performed on seven samples (samples 8-2A, 8-3A-1, 8-3A-2, 8-3A-3, 8-4A, 8-7, 8-8) at the Department of Geochemistry of the Geological Survey of Austria. (Tab. 3b). The samples were first crushed, partitioned and milled (< 60 µm). Desiccation and ignition loss of the air-dried samples at 110° C and 1050° C was gravimetrically analysed. Main and trace elements were determined by X-ray fluorescence, using a X-LAB 2000 SPECTRO. Analyses of additional Rare Earth elements (REE) and selected trace elements were carried out on two samples from the tuffs (sample 8-2A, 8-3A-1; cf. Tab. 3c) using ICP-AES on a Thermo Jarell Ash IRIS Advantage (method A 62) at the laboratory of the Czech Geological Survey in Prague-Barrandov.

3.3 $^{40}Ar/^{39}Ar$ dating

A bulk ash sample was crushed, disintegrated in a calgon solution and afterwards washed and sieved over a set of sieves between 63 and 250 µm. The residue was subjected to standard heavy liquid as well as magnetic mineral separation techniques. The fraction of grains larger than 150 µm contained ample K-feldspar crystals. These were handpicked and leached with a 1:5 HF solution in an ultrasonic bath for 5 min

sample		bulk rock mineralogy (mass %)					clay mineralogy (mass %) fraction < 2 µm		
		quartz	plagioclase	alkali feldspar	phyllosilicates	apatite	smectite	illite	kaolinite
8-4A (tuff)	top	0	1	0	99		99	0	0
8-3A-1 (tuff)		0	1	0	99		99	0	0
8-2A (tuff)		0	1	0	99		99	0	0
8-1A (siltclay)		15	3	1	81		84	14	2
8-7 (tuffite)	base	8	1	0	48	43			

Table 2: Semi-quantitative mineralogical composition of sediments from Straning outcrop; volcanic glass phases not considered.

and subsequently cleaned in distilled water.

The mineral separates were then loaded in a 10 mm ID quartz vial together with Fish Canyon Tuff (FC-2) and Drachenfels (grain size fraction 250-500µm and grain size fraction >500µm) sanidine. The vial was irradiated at the Oregon State University TRIGA reactor in the cadmium shielded CLICIT facility for 10 hours.

Fourteen multigrain splits of the mineral separate were loaded into two copper sample-trays together with Drachenfels as well as Fish-Canyon sanidine standards upon return to the VU Amsterdam laboratory. The trays were pre-heated under vacuum using a heating stage to remove undesirable atmospheric argon. The samples were subsequently placed in the ultra-high vacuum sample chamber and degassed overnight. They were then fused using a Synrad CO_2 laser in combination with a Raylase scanhead as a beam delivery and beam diffuser system. After purification the resulting gas was measured with a Mass Analyser Products LTD 215-50 noble gas mass spectrometer. Beam intensities were measured in peak-jumping mode in 0.5 mass intervals over the mass range 40 - 35.5 on a Balzers 217 secondary electron multiplier. System blanks were measured every three to four steps. Mass discrimination was monitored by frequent analysis of aliquots of air. Uncertainty in the mass discrimination factor amounts was 0.2%. The irradiation parameter J for each unknown was determined by interpolation using a polynomial fit between the individually measured standards. We adopt a very conservative 1% uncertainty in the J-value. All $^{40}Ar/^{39}Ar$ ages were calculated with the in-house developed ArArCalc software (Koppers, 2002), applying the decay constants of Steiger and Jäger (1977). The age for Fish Canyon Tuff sanidine flux monitor used in age calculations is 28.201 ± 0.046 Ma (Kuiper et al., 2008). The age for the Drachenfels sanidine flux monitor is 25.477 ± 0.03 Ma (Mandic et al., 2012). Correction factors for neutron interference reactions are 2.64 ± 0.017 × 10^{-4} for $(^{36}Ar/^{37}Ar)_{Ca}$, 6.73 ± 0.037 × 10^{-4} for $(^{39}Ar/^{37}Ar)_{Ca}$, 1.211 ± 0.003 × 10^{-2} for $(^{38}Ar/^{39}Ar)_{K}$ and 8.6 ± 0.7×10^{-4} for $(^{40}Ar/^{39}Ar)_{K}$. Errors are quoted at the 1σ level.

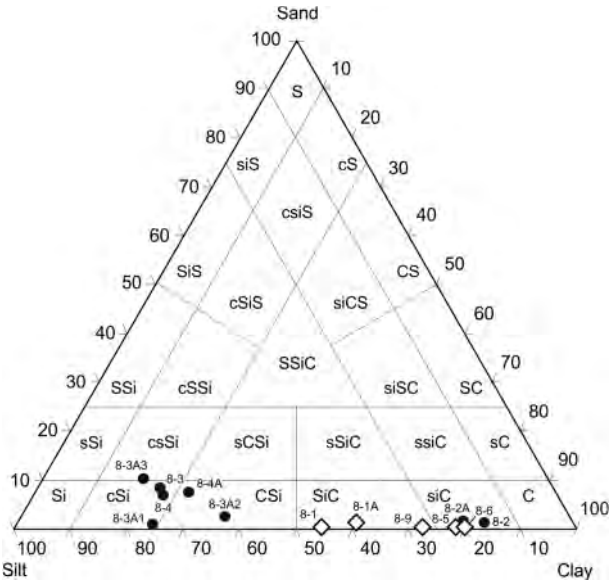

Figure 4: Ternary grain size diagram of the samples from outcrop Straning. Black circles: tuff samples; white rhombs: samples from Zellerndorf Formation below. Nomenclature of the ternary diagram after Füchtbauer (1959) and Müller (1961); abbreviations: S: sand, Si: silt, C: clay, s: sandy, si: silty, c: clayey.

3.4 Palaeomagnetism

Two palaeomagnetic laboratories studied the tuff locality at Straning. The two laboratories worked separately, at different times and used partly similar, partly different methods.

The team of the Palaeomagnetic Laboratory of the Geological and Geophysical Institute of Hungary in Budapest drilled cores with a petrol powered portable drill from the freshly excavated outcrop and oriented them in situ with a magnetic compass. The team of the 'Gams' Palaeomagnetic Laboratory of the University of Leoben collected hand samples, oriented them in situ with a magnetic compass and drilled cores from the hand samples in the laboratory. In the laboratories the cores were cut into 2 cm specimens.

In Budapest, the following instruments and demagnetizers were used: JR-4 and JR-5A (AGICO, Brno) spinner magnetometers to measure remanent magnetization, a KLY-2 Kappabridge (AGICO, Brno) to measure magnetic susceptibility, LDA-3A (peak field: 0.1 T) and DEMAG 0179 (peak field: 0.235 T) alternating field demagnetizers (AGICO, Brno and Technical University of Budapest, respectively) for alternating field demagnetisation, a TSD1 thermal demagnetizer (Schonstedt, Reston) for thermal demagnetization and a pulsmagnetizer (Molspin, Newcastle upon Tyne) for isothermal remanent magnetization experiments. The natural remanent magnetization of the specimens was measured in the natural state. One specimen from each sample was subjected to stepwise alternating field or combined alternating field and thermal demagnetization. The natural remanent magnetization was re-measured after each step, followed by a susceptibility measurement in the case of thermal demagnetization. Isothermal remanent magnetization experiments were conducted for selected specimens.

In Gams, a 2G Enterprises cryogenic magnetometer was used to measure remanent magnetization, a MFK1-FA Multifunction Kappabridge (AGICO, Brno) was used to measure magnetic susceptibility, and MMTD60 and MMTD1 (Magnetic Measurements, Liverpool) thermal demagnetizers were used for thermal demagnetization. The natural remanent magnetization of the specimens was measured in the natural state. One specimen from each sample was subjected to stepwise thermal demagnetization. The natural remanent magnetization was re-measured after each step.

In both laboratories the demagnetization curves were analysed for linear segments through principal component analysis (Kirschvink, 1980). Only components decaying towards the origin were used to calculate the locality mean palaeomagnetic direction (Fisher, 1953).

Sample	SiO_2 (%)	TiO_2 (%)	Al_2O_3 (%)	FeO (%)	Na_2O (%)	K_2O (%)	CaO (%)
8-4A (6)	79.01		12.96	1.25	2.04	4.00	0.71
8-3A-2 (4)	78.74	0.08	12.83	1.16	1.72	4.86	0.62
8-3A-1 (3)	77.40		13.43	1.36	2.41	4.54	0.87
8-7 (3)	78.19		13.18	1.40	2.12	4.30	0.78

Table 3a: CamScan electron microprobe analyses of major elements of the volcanic glass from the Straning outcrop (number of analysed grains in brackets).

4. Results

4.1 Grain size distribution

The grain size analyses show clear differences between the volcaniclastic layers and the underlying sediments (Figs. 2, 4, Tab. 1). The basal deposits of the Zellerndorf Formation (samples 8-5, 8-6) are very fine grained silty clays (nomenclature after Füchtbauer, 1959; Müller, 1961) with a mean of 12.7 to 12.8 Phi (0.15 – 0.14 µm). A first volcanic activity is manifested by a volcaniclastic intercalation (sample 8-7). This layer is conspicuously coarser than the pelitic sediments below. Grain size analysis was, however, not useful because of a high amount of secondary solidified aggregations falsifying the result. The fine grained sediments with thin whitish volcaniclastic layers following above (samples 8-9, 8-1, 8-1A) are siltclays. They show a mean between 12.2 and 10.3 Phi (0.2 – 0.8 µm) and are slightly coarser than the lower pelitic sediments.

The light coloured volcaniclastic layers following above are in most cases completely different in colour and grain size (cf. Fig. 4). They start with relatively fine grained silty clays (samples 8-2, 8-2A) with a mean between 11.8 and 12.1 Phi (0.28 – 0.23 µm). The volcaniclastic sediments that follow (samples 8-3A-1, 8-3, 8-3A-2, 8-3A-3, 8-4, 8-4A) are clearly coarser claysilts, clayey silts, and clayey sandy silts with a variable mean in different beds between 7.1 and 8.6 Phi (7.3 – 2.6 µm).

4.2 Mineralogy

Bulk rock and clay mineralogy analyses were carried out for five samples. Four of these derived from the volcaniclastic sediments, whereas one sample came from the fine grained deposits below (Tab. 2). The XRD measurements were complemented with optical microscopy and grain size analyses that helped to quantify the results, especially that of volcanic glass.

Sample 8-1A from the base of the volcaniclastic deposits is composed of 80% phyllosilicates, 15% quartz and small portions of feldspar. The major clay mineral in the fraction < 2 µm is smectite (84%), besides small amounts of illite (14%) and traces of kaolinite.

The bulk rock mineralogy of the overlying tuffs and tuffites (samples 8-2A, 8-3A-1, 8-4A) consists almost completely of phyllosilicates and minor traces of plagioclase as well as the not measurable volcanic glass. Clay mineralogy analyses only indicate the presence of smectite. Smectite was identified by comparing diffraction patterns of Mg-treated and glycolated preparations. The Mg-treated preparations give very strong 001 reflections at about 5.98 °2Θ , which, in the glycolated states shift to about 5.18 °2Θ.

Sample 8-2A is made up of 80% of minerals smaller than 2 µm and classifies as a bentonite. Inspection of samples from the coarser grained horizons (8-3A-1 and 8-4A) under the microscope revealed that they contain appreciable amounts of silt to fine sand size

Sample	La	Ce	Pr	Nd	Sm	Eu	Gd	Tb	Dy	Ho	Er	Tm	Yb	Lu	Y	Nb	Zr	Rb
8-3A-1	51	103	12	50	10	1	7	< 2	7	2	3	0.6	3	0.4	32	14	309	48
8-2A	55	101	19	42	11	1	6	< 2	7	0.3	3	0.5	3	0.3	29	10	296	27

Table 3c: ICP-AES analyses of Rare Earth elements (REE) and selected trace elements from tuff samples from the Straning outcrop (in ppm).

Sample	SiO_2	TiO_2	Al_2O_3	Fe_2O_3	MnO	MgO	CaO	Na_2O	K_2O	P_2O_5	CO_2	SO_3	H_2O-	H_2O+	Total	CIA	Ba	Co	Cr	Cu	Ga	Mo	Ni	Pb	Sr	V	Zn
8-4A	62.5	0.38	14.0	3.05	0.028	1.6	2.00	1.45	1.90	0.11	0.13	<0.01	6.6	6.3	100.05	27	555	<5	3	9	23	<5	3	30	91	29	65
8-3A-3	64.5	0.31	14.2	2.7	0.28	1.48	1.30	1.70	2.30	0.11	0.13	<0.01	4.6	6.3	99.91	25	760	5	9	15	20	<5	15	28	120	25	84
8-3A-2	56.3	0.37	15.5	3.7	0.014	2.95	1.05	0.75	1.08	0.11	0.13	<0.01	11.3	6.7	99.95	44	320	8	4	7	21	<5	21	18	73	30	63
8-3A-1	53.5	0.43	17.0	3.0	0.023	3.45	0.85	0.57	0.68	0.11	0.13	<0.01	13.2	7.1	100.04	54	225	7	5	10	27	<5	6	19	75	32	67
8-2A	50.8	0.40	17.0	3.5	0.016	3.95	0.70	0.21	0.19	0.11	0.17	0.01	16.1	6.9	100,06	76	88	8	4	10	29	<5	12	<5	53	34	68
8-8	15.0	0.19	4.1	58.0	3.22	0.80	1.20	0.10	0.72	1.20	0.80	<0.01	3.5	10.3	99.13		920	18	5	15	8	<5	270	49	138	42	600
8-7	30.7	0.38	7.9	2.2	0.090	1.15	27.0	0.30	1.33	19.5	2.80	0.01	3.8	2.8	99.96	88	250	<5	45	7	12	<5	11	<5	650	59	65

Table 3b: Bulk rock fluorescent X-ray analyses of tuffs, tuffites, and limonite samples from Straning outcrop. Major elements in weight %, trace elements in ppm, CIA: Chemical Index of Alteration.

Combined experiments	Straning		$^{36}Ar_{(a)}$	$^{37}Ar_{(ca)}$	$^{38}Ar_{(cl)}$	$^{39}Ar_{(k)}$	$^{40}Ar_{(r)}$	Age ± 1s (Ma)	$^{40}Ar_{(r)}$ (%)	$^{39}Ar_{(k)}$ (%)	K/Ca ± 1s	$^{39}Ar_{(k)}/^{40}Ar_{(a+r)}$ ± 1s	$^{36}Ar_{(a)}/^{40}Ar_{(a+r)}$ ± 1s
09M0215E	7.00 W		0.000190	0.032469	0.000491	0.316923	1.122300	17.02 ± 0.14	95.21	0.81	4.197 ± 0.149	0.268923 ± 0.001064	0.000161 ± 0.000024
09M0132O	7.00 W		0.001365	0.155204	0.000680	3.245846	11.591432	17.16 ± 0.07	96.61	8.26	8.993 ± 0.185	0.270603 ± 0.000999	0.000114 ± 0.000003
09M0215D	7.00 W	•	0.000388	0.041723	0.000845	1.648411	5.922509	17.26 ± 0.05	98.08	4.19	16.988 ± 0.574	0.273050 ± 0.000723	0.000064 ± 0.000004
09M0215C	7.00 W	•	0.000374	0.044549	0.000000	1.374054	4.949666	17.31 ± 0.06	97.79	3.50	13.263 ± 0.439	0.271546 ± 0.000835	0.000074 ± 0.000006
09M0215A	7.00 W	•	0.000633	0.128812	0.000019	2.427574	8.745701	17.31 ± 0.06	97.88	6.18	8.104 ± 0.260	0.271763 ± 0.000833	0.000071 ± 0.000004
09M0132F	7.00 W	•	0.001313	0.165199	0.000595	3.015000	10.875688	17.33 ± 0.07	96.53	7.67	7.848 ± 0.162	0.267676 ± 0.001015	0.000117 ± 0.000003
09M0132P	7.00 W	•	0.001903	0.196207	0.000000	5.594600	20.290958	17.43 ± 0.05	97.28	14.24	12.261 ± 0.240	0.268284 ± 0.000666	0.000091 ± 0.000003
09M0132M	7.00 W	•	0.001611	0.139305	0.000068	2.127339	7.719560	17.44 ± 0.06	94.17	5.41	6.567 ± 0.130	0.259570 ± 0.000799	0.000197 ± 0.000006
09M0132E	7.00 W	•	0.001488	0.141726	0.000037	2.778380	10.082320	17.44 ± 0.06	95.80	7.07	8.430 ± 0.168	0.264053 ± 0.000840	0.000141 ± 0.000003
09M0132N	7.00 W	•	0.002292	0.156695	0.000000	4.225685	15.357764	17.46 ± 0.05	95.75	10.75	11.596 ± 0.230	0.263529 ± 0.000676	0.000143 ± 0.000004
09M0132D	7.00 W		0.001194	0.146261	0.000000	3.107794	11.354163	17.55 ± 0.05	96.96	7.91	9.137 ± 0.179	0.265466 ± 0.000760	0.000102 ± 0.000004
09M0132G	7.00 W		0.001153	0.157004	0.000219	2.972412	10.909792	17.63 ± 0.06	96.95	7.56	8.141 ± 0.164	0.264200 ± 0.000890	0.000103 ± 0.000003
09M0132B	7.00 W		0.001592	0.153661	0.000000	3.271631	12.091975	17.76 ± 0.07	96.23	8.33	9.155 ± 0.184	0.260429 ± 0.000986	0.000127 ± 0.000003
09M0132A	7.00 W		0.001496	0.122814	0.000000	3.191829	12.505475	18.82 ± 0.06	96.57	8.12	11.175 ± 0.217	0.246520 ± 0.000720	0.000116 ± 0.000004

Summary $^{40}Ar/^{39}Ar$ data Straning
VU-ID: VU78-15
Location: Straning
N: 8, N_{tot}: 14

$^{40}Ar^*/^{39}Ar_K$ ± 1s: 3.6164 ± 0.0058
Weighted mean age (Ma) ± 1s (analytical): 17.38 ± 0.03
Weighted mean age (Ma) ± 1s (total error): 17.38 ± 0.18
MSWD: 2.02

$(^{40}Ar/^{39}Ar)_{atm}$ ± 1s: 369 ± 26

Inverse isochron age (Ma) ± 1s (analytical): 17.23 ± 0.06
Inverse isochron age (Ma) ± 1s (total error): 17.23 ± 0.18
MSWD: 0.95
J VU78-15 = 0.0026762 ± 0.0000268
J relative to FC = 28.201 ± 0.028 Ma

volcanic glass. Grain size analyses indicate the proportion of clay in these samples to be less than 30%. Thus, it might be assumed that the portions of smectite are approximately in the same range (Tab. 1 and 2).

The tuffitic intercalation in the basal sediments (sample 8-7) shows a different mineralogy. This coarser layer is characterised by 48% of phyllosilicates (29% smectite, 10% muscovite, 6% illite, 3% chlorite), 8% quartz and 1% plagioclase. On top of that there is a remarkable 43% apatite component.

Large amounts of translucent and milky glass, as well as biotite, alkali feldspar, plagioclase, quartz, ilmenite, apatite, and zircon were identified in the tuffs and tuffites under the microscope by SEM- and EDS-studies. Apatite and ilmenite frequently occur as idiomorphic crystals, the latter also as metallic glossy spherules or with incomplete crystal faces (Fig. 5d). Quartz spherules were frequently found (Fig. 5f), and in some cases show initial stages of crystal faces turning into euhedral, hexagonal, bipyramidal quartz. These types of quartz were also described in older tuffitic layers in drillings from Niederfladnitz (Roetzel et al., 1994) and Pulkau (Schubert et al., 1999).

4.3 Tephrostratigraphy

Our tephrostratigraphic study is based on point wise microprobe investigation of volcanic glass from the tephra, on zircon studies as well as on whole-rock geochemical analyses.

4.3.1 Volcanic glass and bulk rock geochemistry

The investigation of volcanic glasses is an essential part of tephra studies. The major element geochemistry of volcanic glasses from the Straning tuffs is given in Tab. 3a. According to the TAS diagram (Le Maitre, 1984) the studied volcanic glasses classify as rhyolite glasses (Fig. 6a). The K_2O vs. SiO_2 diagram (Le Maitre et al., 1989) indicates that the glasses originated from calc-alkaline volcanism (Fig. 6b).

The chemistry of the volcanic glass is comparable with the results of the bulk rock chemistry (Tab. 3b and 3c). The calc-alkaline origin of the tuffs is confirmed by the position of the results for samples 8-4A, 8-3A-3, 8-3A-2, and 8-3A-1 in the AFM diagram (Fig. 6c). Moreover, the geochemistry of

Table 4: Most relevant analytic data for the dated Straning tuff. Dots (•) mark measurements used for calculation. The full analytical data are provided in the supplementary material.

samples 8-2A and 8-3A-1 also confirms a rhyodacitic/dacitic character of the volcanic source in the classification diagram Zr/TiO_2 vs. Nb/Y (Winchester and Floyd, 1977; Fig. 6d). The position of the obtained results in Nb vs. Y and Rb vs. Y+Nb discrimination diagrams for acidic magmatic rocks (Pearce et al., 1984) furthermore suggests that the tuffs originated from calc-alkaline arc volcanism (Figs. 6e and 6f). The ratio of Zr/Nb varies between 22.1 and 29.6 which can be interpreted to reflect a post-collisional setting. It is indicative of a high-K calc-alkaline series produced by arc-related volcanism (Leat et al., 1986).

The chondrite-normalized REE patterns for Straning tephra samples (Fig. 6g) are very similar for the two studied samples (La_N/Yb_N = 10.98 and 13.12). The slope of LREE is slightly steeper (La_N/Sm_N = 3.11 and 3.22) compared to a more gentle HREE slope (Gd_N/Yb_N = 1.82 and 1.87). The general pat-

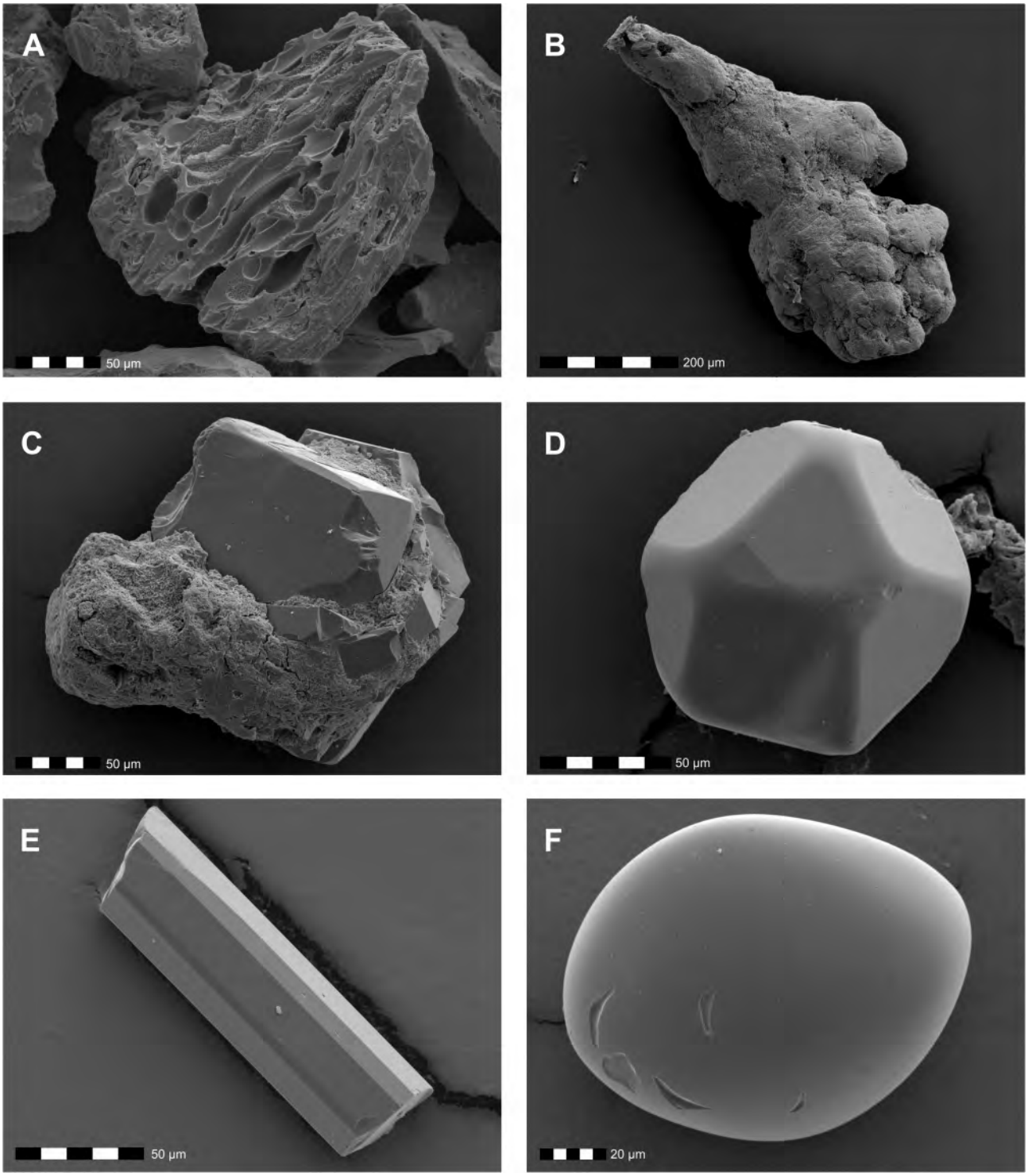

Figure 5: SEM microphotos of components from the Straning tuff (A: sample 8-3A-3; B, C, D: sample 8-2; E, F: sample 8-2A). A: glass components, B: air-formed slag, C: plagioclase in slag, D: idiomorphic ilmenite, E: idiomorphic apatite, F: quartz spherule.

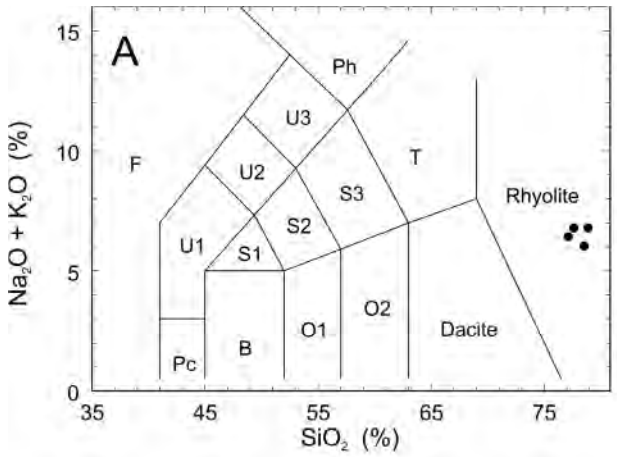
A
Ph
U3
F
U2
T
S3
Rhyolite
U1
S1
S2
O1
O2
Dacite
Pc
B
$Na_2O + K_2O$ (%)
SiO_2 (%)

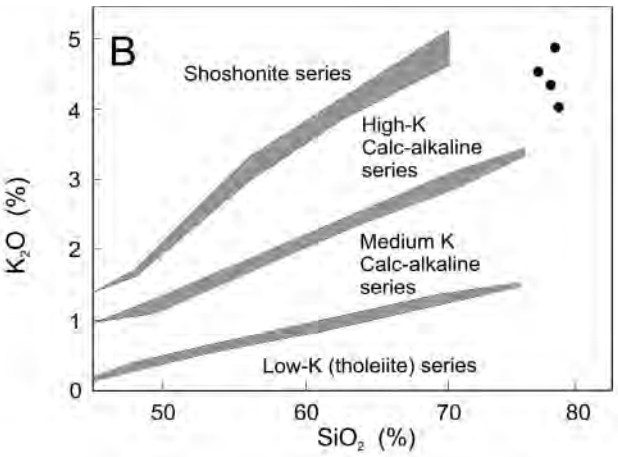
B
Shoshonite series
High-K
Calc-alkaline
series
Medium K
Calc-alkaline
series
Low-K (tholeiite) series
K_2O (%)
SiO_2 (%)

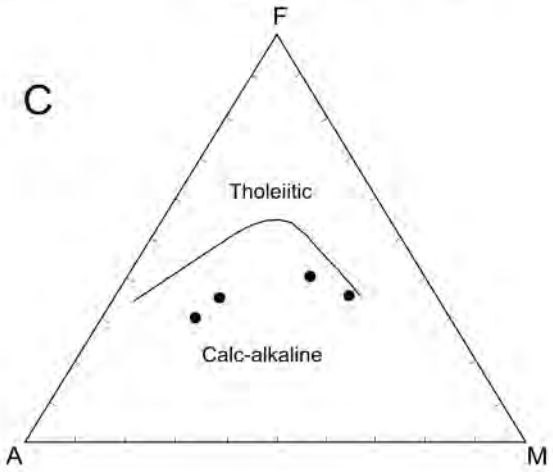
C
F
Tholeiitic
Calc-alkaline
A
M

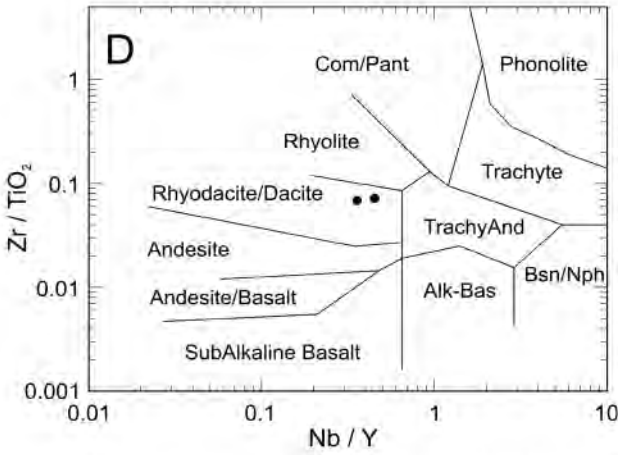
D
Com/Pant
Phonolite
Rhyolite
Trachyte
Rhyodacite/Dacite
TrachyAnd
Andesite
Bsn/Nph
Andesite/Basalt
Alk-Bas
SubAlkaline Basalt
Zr / TiO_2
Nb / Y

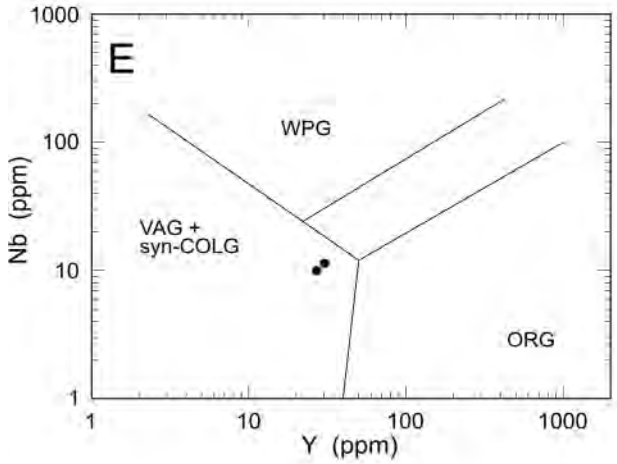
E
WPG
VAG +
syn-COLG
ORG
Nb (ppm)
Y (ppm)

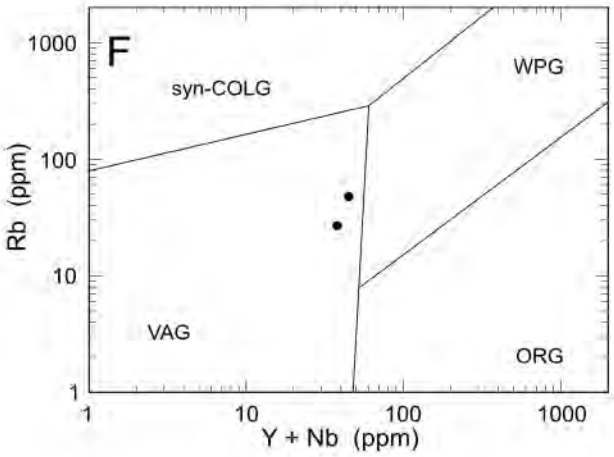
F
syn-COLG
WPG
VAG
ORG
Rb (ppm)
Y + Nb (ppm)

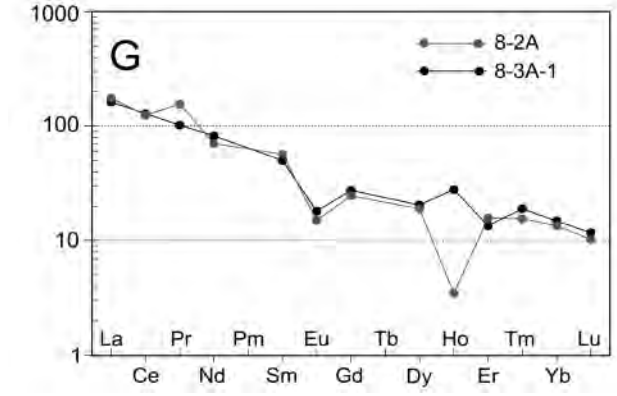
G
8-2A
8-3A-1
La
Ce
Pr
Nd
Pm
Sm
Eu
Gd
Tb
Dy
Ho
Er
Tm
Yb
Lu

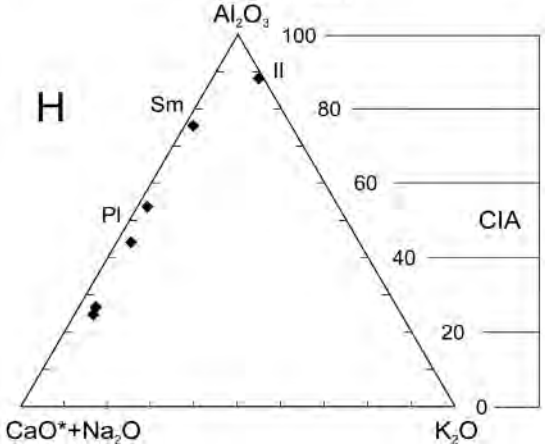
H
Al_2O_3
Il
Sm
Pl
CIA
CaO^*+Na_2O
K_2O

terns of the curves tend to be characteristic for acidic granitic respectively rhyolitic magmas. The Eu-anomaly is moderately developed and the Eu/Eu* indexes are 0.40 and 0.49, which can be interpreted as plagioclase depletion of a parental magmatic melt.

An estimate of the degree of alteration of volcanic material can be obtained by calculating the CIA (Chemical Index of Alteration: Nesbitt and Young, 1982, Fedo et al., 1995, Roy et al., 2008). The CIA values of the Straning tuff samples (except sample 8-8 – limonitic layer) are presented in Tab. 3b and Fig. 6h. The CIA index of the Straning tuffs increases from the top to the bottom of the outcrop, which indicates a downwards increase in chemical weathering (hydrolysis), especially of volcanic glass (depletion of Na, K, Ca, and Si) and progressive transformation into clay minerals (increase of Al and also Mg).

The CIA values of the Straning tuff samples follow a distinct linear trend parallel to the A-CN join in the A-CN-K plot (Fig. 6h), with the exception of sample 8-7. The linearity of this trend suggests that the corresponding tuffs had a common source rock composition but experienced various degrees of chemical weathering. The CIA value of sample 8-7 clearly deviates from the trend, which indicates that it originated from a different parent material. This is in line with the mineralogical results of sample 8-7 with an extremely high apatite content (cf. Tab. 2) and the bulk rock geochemical results with very high P, Cr and Sr (cf. Tab. 3b). On the other hand, the relative enrichment of smectite in sample 8-2A and plagioclase in samples 8-3A-2 and 8-3A-1, which is reflected in the position of these samples in the A-CN-K diagram, is not as clearly expressed in the semi-quantitative mineralogical results provided in Table 2.

4.3.2 Zircon studies

A total population of 480 zircons from tuff samples 8-2A, 8-3, 8-3A-1, 8-3A-2, and 8-4A was studied. Among these zircons, euhedral grains are dominant (70.0% to 96.4%). Subhedral grains comprise about 1.8% to 26.7% and rounded grains about 0% to 5.3% of the zircon population (Fig. 7a). There is also a variation in the outer morphology of zircons between samples. These differences reflect variations in the proportions of volcanic and non-volcanic material in the studied samples as well as a varying influence of secondary transport/redeposition (i.e. after the fallout) and mixing.

The proportion of (sub)euhedral zircons varies from 81.2% to 97.3% of the studied grains. The zircons show a broad variety of surface textures and different textures even occur on single zircon crystals. Glass coating of the zircon grains is common. Irregular crystal intergrowths in various stages of disintegration, complicated and numerous build-ups of smaller crystals, broken crystals, irregular and rough crystal faces, irregularities of crystal planes and edges were also observed. These structures evolved both within the stratified magma chamber and within the tephra cloud (Kowallis et al., 1989). A polyphase generation of the zircons is also reflected in their crystallographic development; opposite pyramids or prisms are frequently present in single zircon crystals. Furthermore, numerous euhedral crystals of apatite were present in the studied samples; particularly in 8-3A-1 and 8-3A-2 (cf. Fig. 5e). Apatite strongly dominates over zircon.

Internal zonation and the presence of inherited cores and inclusions within the grains are important features of the inner fabric of zircons in general. Neither zircons with elder cores nor zircons with zonality were observed in the studied samples, suggesting that they formed rapidly. Zircons with inclusions are, on the other hand, very abundant. They form 98.2% to 100% of the zircon population. The shape, dimension and orientation of inclusions vary.

The elongation of the studied zircons is very variable (results from 339 zircons). The average value of elongation differs for various samples and ranges between 2.6 and 3.4. The maximum value of elongation also varies and ranges between 4.4 and 12.6. Zircons with an elongation over 3 represent 21.5% to 30.9% and zircons with an elongation over 4 make up 4.3% to 20.6% of the whole zircon population. These “highly elongated” zircons are interpreted to be typically volcanic ones (Zimmerle, 1979). A higher value of elongation was recognised mainly for the long prismatic crystals with relatively reduced pyramids. Fragments of prisms also occur in the studied samples. Differences in the average value of elongation and in the proportion of “highly elongated” zircons in different samples from Straning reflect differences in the proportion of volcanic material and also the different degrees of redeposition in individual samples.

Volcanic zircons of typological types S_{23}, S_{24}, S_{22}, and S_{17} are dominant in the Straning tuff. The position of the “typology mean point” in the diagram of Pupin (1985) provides evidence of the origin of the parental magma and can also be effectively used for tephrostratigraphic correlations (Kowallis et al., 1989; Kowallis and Christiansen, 1990; Nehyba and Roetzel, 1999; Nehyba et al., 1999). In the case of the Straning tuffs, the parental magma had a hybrid character (i.e. mixing of mantle and crustal magmas – Pupin, 1980, 1985), slightly closer to anatectic in origin (Fig. 7b). The position of the “typology mean

Figure 6: 6a: TAS (total alkali silica) classification diagram for volcanic glass from Straning (diagram after Le Maitre, 1984); abbreviations: B - basalt, F - foidite, O1 - basaltic andesite, O2 - andesite, Pc - picrobasalt, Ph - phonolite, S1 - trachybasalt, S2 - basaltic trachyandesite, S3 - trachyandesite, T - trachyte, U1 - basanite, U2 - phonotephrite, U3 – tephro-phonolite. 6b: K_2O vs. SiO_2 diagram for volcanic glass from Straning (diagram after Le Maitre et al., 1989). 6c: AFM diagram for tuffs from Straning ($A=Na_2O+K_2O$, F=FeO, M=MgO, diagram after Irvine and Baragar, 1971). 6d-6f: Trace element discrimination diagrams for Straning volcaniclastics (6d: diagram after Winchester and Floyd, 1977; 6e, 6f: diagram after Pearce et al., 1984); abbreviations: Com/Pant - Comendite/Pantellerite, Bsn/Nph - Basanite/Nephelite, Alk-Bas - Alkaline-Basalt, ORG - ocean ridge granites, VAG - volcanic arc granites, WPG - within plate granites, syn-COLG - syn-collision granites. 6g: Chondrite-normalized REE patterns (Boynton, 1984) for the studied Straning volcaniclastics. 6h: A-CN-K diagram and corresponding CIA values for samples from Straning ($A=Al_2O_3$, $CN=CaO^*+Na_2O$, $K=K_2O$). The diagram also represents the fields of idealised minerals (Pl – plagioclases, Il – illite, Sm – smectite).

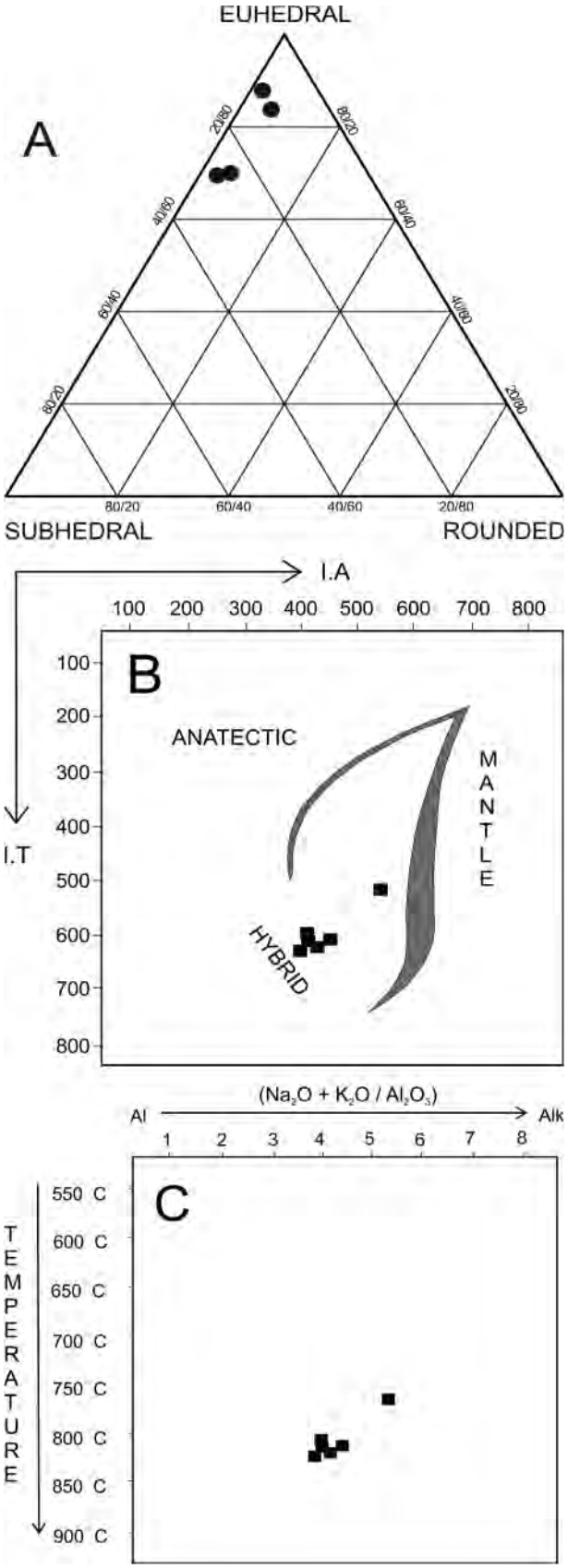

Figure 7: 7a: Ternary diagram of euhedral, subhedral and rounded zircons in the studied samples. 7b: Plot of average Pupin indices for the studied volcanic zircons (diagram after Pupin, 1980, I.T. and I.A. values are typology coordinates of the development of prisms and pyramids of zircons (Pupin, 1980). 7c: Mean point distribution in the main domains of the typologic diagram for the studied volcanic zircons (diagram after Pupin, 1985).

point" generally reveals a high I.T. value (typology coordinates of the development of prisms of zircons) (above 800° C), and a relatively low content of alkaline elements (I.A. value; typology coordinates of the development of pyramids of zircons) for the studied samples (Fig. 7c).

4.4 $^{40}Ar/^{39}Ar$ geochronology

A summary of the results of the $^{40}Ar/^{39}Ar$ total fusion experiments on K-feldspar grains from the Straning tuffs is given in table 4. A comprehensive table is also provided in the supplementary material. The total fusion age of all conducted experiments combined is 17.55 ± 0.18 Ma. A weighted mean age of 17.38 ± 0.18 Ma is calculated based on 8 out of the 14 measurements that were selected, aiming for a mean square weighted deviation (MSWD) lower than the T-student distribution at the 95% confidence level (Tab. 4, Fig. 8a).

The 369.3 ± 26.2 inverse isochron intercept nevertheless deviates from the atmospheric argon ratio of 295.5. This is interpreted to reflect excess argon. We therefore regard the 17.23 ± 0.18 Ma inverse isochron age (Fig. 8b) as the best estimate for the age of the ash layer.

The spread evident in the age distribution of individual measurements might be caused by the presence of a small reworked component, not uncommon in these kinds of tuffs, and is also reflected in the tuffs zircon morphology. Taking that into account, the calculated age might slightly overestimate the age of the Straning ash and should be regarded as a maximum estimate. The uncertainty includes uncertainties in J, the age of the primary standard and decay constants, as reported in Kuiper et al. (2008) and Steiger and Jäger (1977) respectively.

4.5 Palaeomagnetism

A common mean direction test (McFadden and McElhinny, 1990) was used to compare the locality mean palaeomagnetic directions obtained in Gams and in Budapest. The test is positive with an 'A' classification, with a γ of 4.43°. The critical γ is 8.09°and consequently the results obtained in the two laboratories are statistically the same and may be combined. The resulting locality mean palaeomagnetic direction for Straning is Declination 163°, Inclination -41° with excellent statistical parameters (k = 112, α_{95} = 3°) (cf. Fig. 9).

In the outcrop the tuff is obviously tilted to E-SE (106/23). When corrected for this tilt, the minimum axis of the AMS fabric approaches the vertical. As this tilt resulted from a landslide, the palaeomagnetic direction after tilt correction cannot be considered useful for tectonic interpretation. Nevertheless, it is important to note that the palaeomagnetic direction both before and after tilt correction has a reversed polarity which is useful for magnetostratigraphic purposes.

5. Discussion

5.1 Regional stratigraphic position and age

The tuffs and tuffites from the Straning outcrop at the south-eastern margin of the Bohemian Massif are an erosion relict

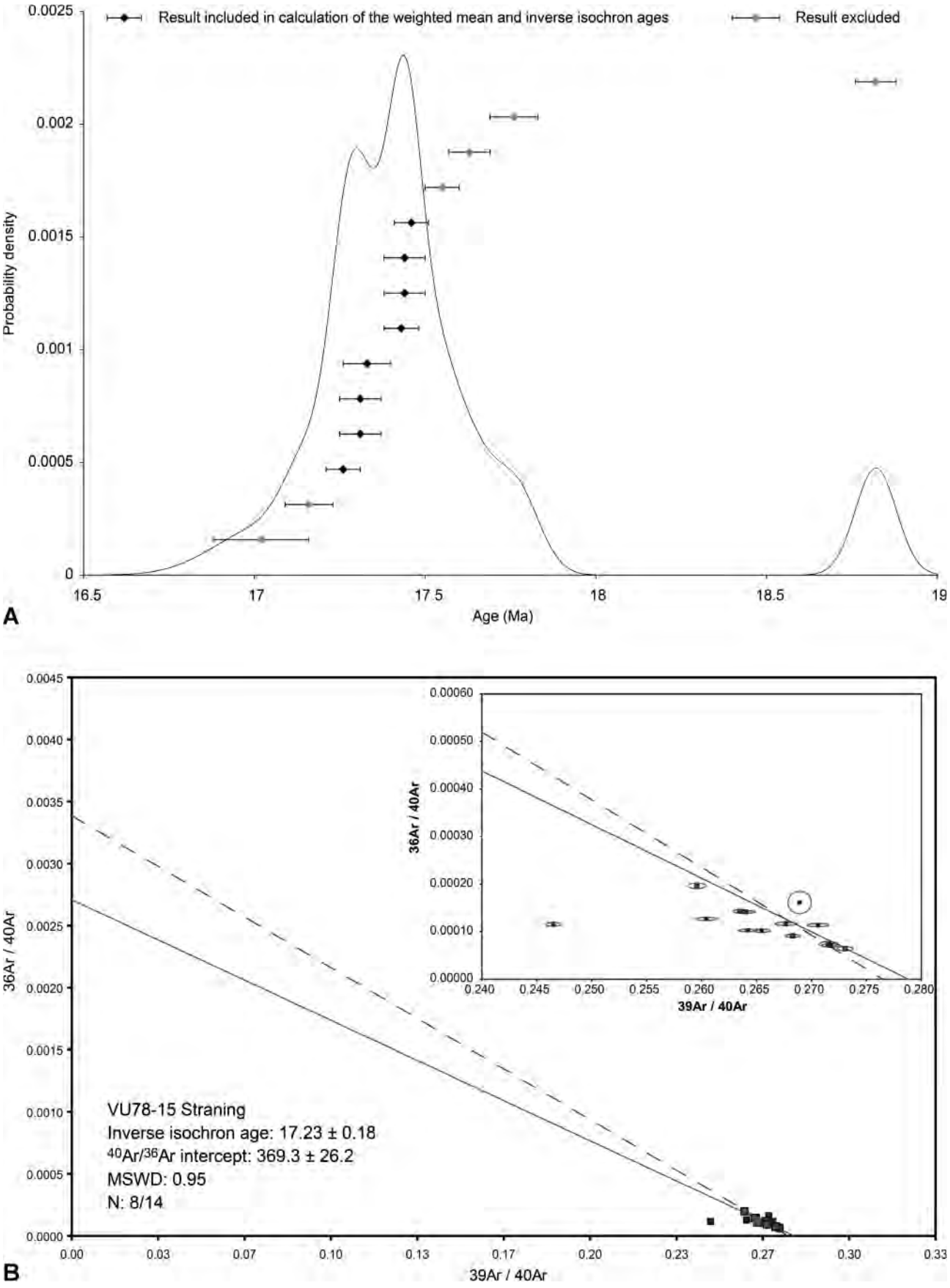

Figure 8: 8a: Probability density distribution for the multiple grain $^{40}Ar/^{39}Ar$ fusion experiments on Straning feldspar. 8b: Inverse isochron diagram of multiple grain $^{40}Ar/^{39}Ar$ fusion experiments on Straning feldspar. The inset shows the data in more detail. The solid line is the inverse isochron line and the dashed line is a reference line based on the weighted mean age (17.38 ± 0.18Ma) and a $^{40}Ar/^{36}Ar$ intercept value equal to the modern atmosphere (295.5). The ellipses in the inset represent the 1σ analytical error. MSWD: mean square weighted deviation, N: number of measured grains. Grey squares represent results selected for age calculation. Black squares represent results that were omitted.

in a small-scale graben within granites of the Thaya-Batholith. The primary tectonic graben existed before the sedimentary filling, as shown by corestone-weathering and limonitic crusts (tafoni-weathering) on the granite surface.

Before the ash-fall the major part of the graben was filled by greenish-grey, thin and plane bedded, non-calcareous, smectitic silty clays of the middle Burdigalian (Ottnangian) Zellerndorf Formation (Roetzel et al., 1999b). The uppermost part of these clays already shows thin tuffitic intercalations. The almost monospecific microfauna (predominantly *?Silicoplacentina* sp. (*"Saccamina"*) and very rare *Triloculina* sp.) in this upper section is typical for shallow, probably brackish-water deposits. The shallow depositional environment may also explain the preservation of the thick acidic volcaniclastics above. The stratigraphic position of the dated ash bed of Straning on top of the Zellerndorf Formation suggests that it is of middle Burdigalian (Ottnangian) or younger age.

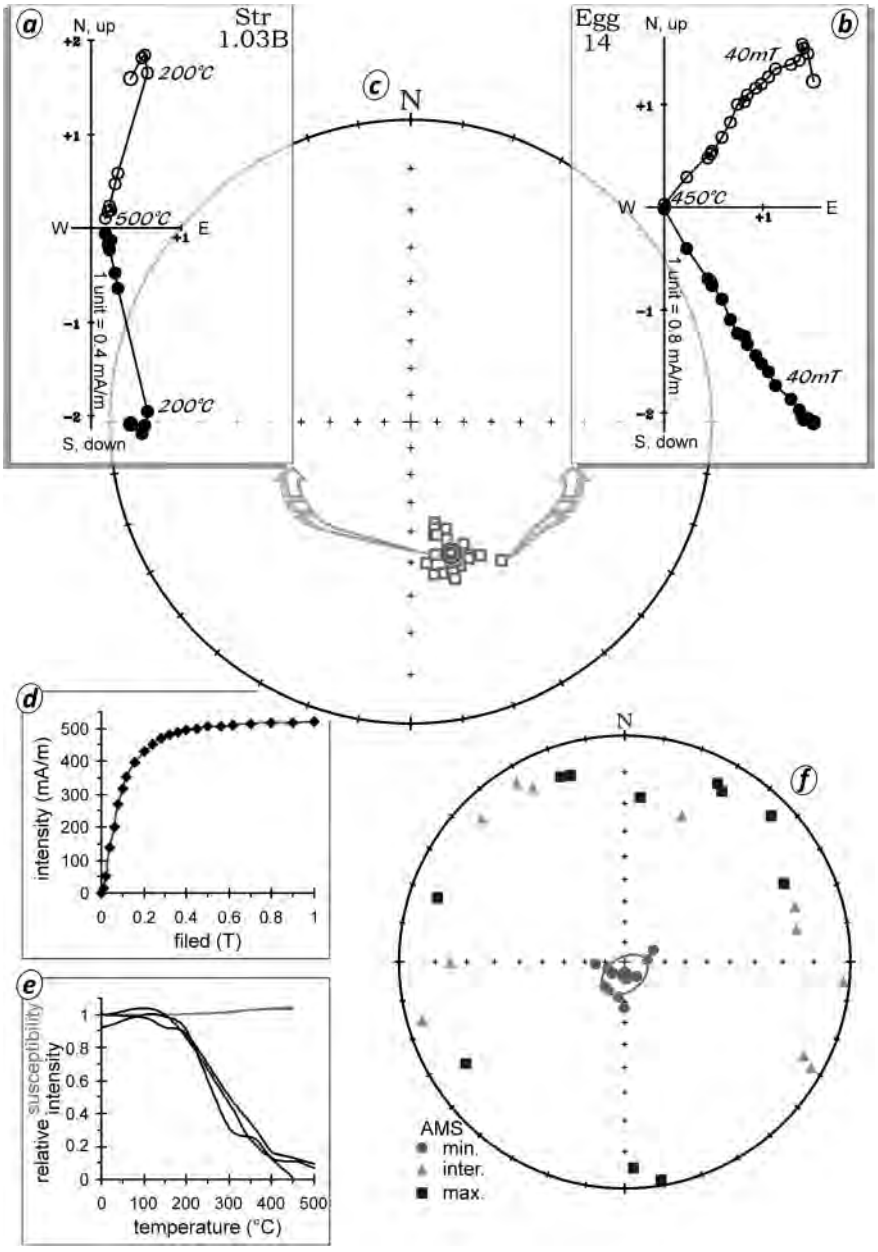

Figure 9: Tuff, locality Straning. Typical Zijderveld (1967) diagrams in geographical system (a and b). Palaeomagnetic directions and locality mean direction with α_{95} on stereographic plot (upper hemisphere) in geographical system (c). Typical isothermal remanent magnetization acquisition curve (d). Natural remanent magnetization (NRM) intensity (black) and susceptibility (grey) curves on thermal demagnetization (e). The orientation of magnetic fabric within the locality. The 95% confidence regions around the principal susceptibility axes (Chadima and Jelínek, 2008) is indicated by ellipses, stereographic plot, tectonic system (f). The acquisition behaviour of the isothermal remanent magnetization (d) indicates that the dominant magnetic mineral is soft, but magnetically hard components are also present. The decay characteristics of the NRM intensity (d) and susceptibility (e) on thermal demagnetization indicates that the actual carrier of the NRM must be a magnetite phase. Key to the Zijderveld diagrams: full dots: projection of the NRM vector onto the horizontal, circles: into the vertical. Str1.03B thermal demagnetization (a), Egg14 combined alternating field and thermal demagnetization (b).

About 90 cm thick acidic tephra-layers are preserved on top of the clays of the Zellerndorf Formation. Apart from the strongly weathered clayey base of the volcaniclastic horizon, the multiphase Straning ash shows a relatively constant silty grain-size with a fine silty mean between 7.1 and 8.6 Phi (7.3 – 2.6 µm) typical for distant fallout tephra. The tephra consists of high amounts of volcanic glass as well as biotite, alkali feldspar, plagioclase, quartz, ilmenite, apatite, and zircon.

A rhyodacite/dacite character of the volcanic source can be deduced from geochemical analyses of the volcanic glass from the Straning tephra. The ash is interpreted to have originated from calc-alkaline arc volcanism. The abundance of zircons of types S_{23}, S_{24}, J_3 and J_4 is indicative of very high eruption temperatures of about 850° C (Kowallis et al., 1989; Kowallis and Christiansen, 1990). The typology of the volcanic zircons also reveals a hybrid character of the parental magma, close to an anatectic origin.

Our geochronological results provide a new age for the Straning tuff. The tuff was previously dated using the $^{40}Ar/^{39}Ar$ method by S. Scharbert (in Roetzel et al., 1999b), who obtained a 16.6 Ma age for weathered biotite crystals with a high content of atmospheric argon and a 16.6 ± 1.0 Ma age for volcanic glass. It is not documented which standard (flux monitor) was used to calibrate these ages against, which makes it impossible to compare them with other $^{40}Ar/^{39}Ar$ ages, including the

new $^{40}Ar/^{39}Ar$ age for the Straning tuff reported here.

Our $^{40}Ar/^{39}Ar$ results for K-feldspar crystals from the Straning tuff indicate an age of 17.23 ± 0.18 Ma. The tuff is therefore attributed to the Late Burdigalian. The indicated age interval corresponds with the middle – late Burdigalian (Ottnangian – Karpatian) transition as well as with the chron C5Dn - C5Cr boundary, which is dated at 17.235 Ma (Gradstein et al., 2012; Fig. 10).

The reversed palaeomagnetic polarity of the tuff restricts the age interval to the lowermost part of the chron C5Cr (base: 17.235, top: 16.721 Ma; Gradstein et al., 2012) and therefore per definition to the basal part of the late Burdigalian (early Karpatian) (Piller et al., 2007). Consequently the volcaniclastics can be correlated with the lowstand systems tract (LST) in the basal part of the global 3rd order sea level cycle Bur 4 of Hardenbol et al. (1998) (Fig. 10).

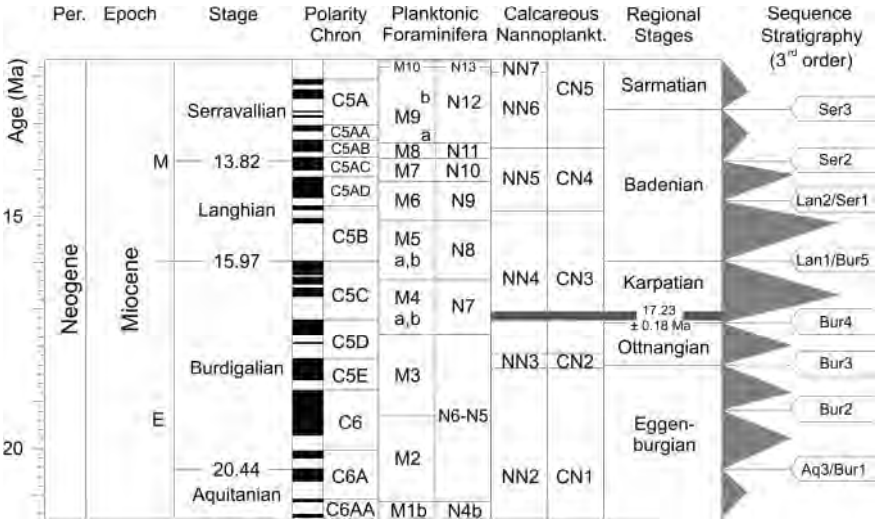

Figure 10: Stratigraphic position of the Straning tuff with geochronology, geomagnetic polarity chrons, biozonations of planktonic foraminifera, and calcareous nannoplankton (all after Gradstein et al., 2012), and sea level curve (after Hardenbol et al., 1998; Piller et al., 2007).

So far, most of the reported acidic tuffs and tuffites from the south-eastern margin of the Bohemian Massif in Lower Austrian and South Moravia were found in lower to middle Burdigalian (Eggenburgian-Ottnangian) deposits. They were dated by biostratigraphy and the zircon fission-track method (Čtyroký, 1982, 1991; Čižek et al., 1990; Nehyba, 1997; Nehyba and Roetzel, 1999; Nehyba et al., 1999; Schubert et al., 1999; Roetzel et al., 1994, 2008).

Thin intercalations (max. few cm thick) of acidic volcaniclastics are also known from the lower Badenian from some drillings in the southern part of the Carpathian Foredeep in Moravia (Nehyba, 1997). They are, however, very rare in this area. Lower Badenian volcaniclastics become distinctly more common in the northern and the middle parts of the foredeep in Moravia with a maximum thickness of up to 7 m (Jurková and Tomšík, 1959; Krystek, 1959, 1983).

The tephra from Straning differs, however, from all previously studied tephra beds in the Carpathian Foredeep in bulk rock geochemisty, volcanic zircon typology, and geochronologic age (cf. Nehyba, 1997; Nehyba and Roetzel, 1999; Nehyba et al., 1999; Nehyba, 2000; Nehyba and Stráník, 2005). The occurrence of this type of volcaniclastics from the late Early Miocene is unique in this area.

The distribution of REE and the content of some other elements of the Straning tuff are quite different from those of Middle Miocene (lower and middle Badenian) tephra from the Carpathian Foredeep (Nehyba, 1997, 2000) and the Langhian (lower Badenian) ones in particular are also clearly distinct with regard to the zircon results (Nehyba, 1997). The latest Langhian to Serravallian (middle Badenian) tuffs also display

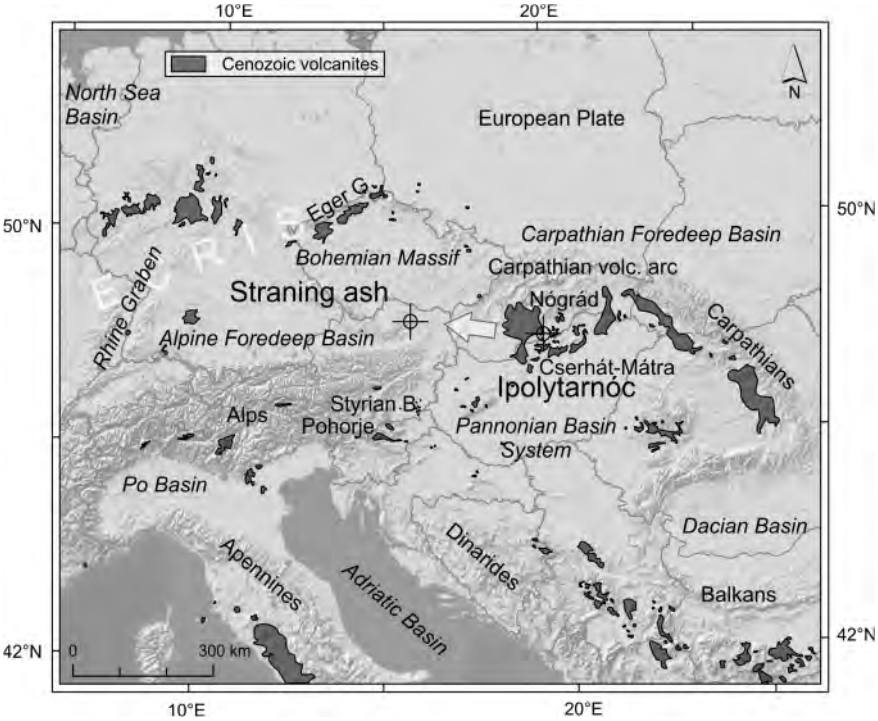

Figure 11: Position of the studied locality and the distribution of Cenozoic volcanic rocks in central Europe. Arrow shows the supposed transport direction of the Straning ash from the western Inner Carpathian volcanic arc. Geology is based upon GISEurope 1:1.5M Bedrock and Structural geology Map, with the permission of OneGeology, geography is based on ArcGIS online base maps by ESRI. ECRIS – European Cenozoic Rift System.

strikingly different zircon I.A values, even though their I.T values are comparable (Nehyba, 2000). Although there are similarities between REE concentrations of the Straning tuff and some Lower Miocene (Eggenburgian and Ottnangian) tephra of the Alpine-Carpathian Foredeep, the I.T. and I.A. values (Pupin, 1980) of these tuffs are very different (Nehyba and Roetzel, 1999). The observed I.T. values for zircons from Straning moreover indicate the highest eruptional temperatures reported for Neogene volcaniclastics in this area. Remarkable is also the presence of zircon typological types J_2 and J_3 observed in some samples from Straning. These types are absent in lower Badenian volcaniclastics from the Carpathian Foredeep but they were observed in the „Krzywe tuff" in the upper Krosno Beds in Poland by Wieser (1985). He described typological types S_{22}, S_{23}, J_3, J_4, and S_{24} as typical for these tuffs.

5.2 Provenance of the Straning ash

Europe experienced strong volcanic activity during the Neogene. Large amounts of volcanic rocks accumulated i.a. in the European Cenozoic Rift System, in the Carpathian–Pannonian region, in the Central Mediterranean, in the Dinarides and Rhodope, and in the Aegean–Anatolia region (Harangi et al., 2006; Seghedi and Downes, 2011) (Fig. 11). Explosive products from this volcanism intercalate with sedimentary rocks in many of the Central and South-eastern European basins. For example, well known Miocene ash intercalations occur in the Alpine-Carpathian Foredeep (Unger and Niemeyer, 1985; Unger et al., 1990; Čižek et al., 1990; Nehyba, 1997; Nehyba and Roetzel, 1999; Kempf and Pross, 2005; Abdul Aziz et al., 2008, 2010; Bukowski et al., 2010; De Leeuw et al., 2010), the East Alpine Basins (Ebner et al., 2002), the Pannonian Basin (Szakács et al., 1998; Pūspōki et al., 2005; Handler et al., 2006; Mandic et al., 2012), Transylvanian Basin (Bedelean and Mârza, 1991; Szakács et al., 2012; De Leeuw et al., 2013), the Dinaride Basins (De Leeuw et al., 2012; Šegvić et al., 2014) and the Apennine Foredeep (Montanari et al., 1994; Krijgsman et al., 1997; Hüsing et al., 2009). More precisely, ashes broadly equivalent in age to the Straning tuff, i.e. late Burdigalian to early Langhian (Karpatian – Badenian) in age, occur in the coal bearing strata in the Styrian Basin (Oberdorf-Voitsberg) and along the Mur-Mürz fault system (Fohnsdorf) (Ebner, 1981; Ebner et al., 1998, 2002; Steininger et al., 1998; Strauss et al., 2003; Hölzel and Wagreich, 2004).

The composition and age of the ash deposits from the Straning outcrop provide indications as to where it's likely source may have been located. There are three potential source areas with volumetrically significant Miocene volcanic activity in Central Europe; (1) the Eger Graben, (2) the Styrian Basin and Pohorje region, and (3) the Inner Carpathian arc at the northern margin of the Pannonian Basin System. The alkaline volcanism of the Eger Graben (Czech Republic) of the European Cenozoic Rift System (ECRIS in Fig. 11) had a peak activity between 18.2 and 16.3 Ma (Wilson and Downes, 1992; Lustrino and Wilson, 2007; Reischmann and Schraft, 2009). It can nevertheless be excluded as a potential source area, because the Straning volcaniclastics are calc-alkaline, rhyodacitic to dacitic, in composition (Fig. 6). Derivation from a Styrian Basin source is not probable either because the production of felsic calc-alkaline material there is confined to the Langhian and early Serravallian (Badenian) and thus does not coincide in time with genesis of the Straning tuff (Steininger and Bagdasarjan, 1977; Poultidis and Scharbert, 1987; Balogh et al., 1994; Pécskay et al., 2006; Trajanova and Pécskay, 2006). The shallow intrusive Pohorje pluton in northern Slovenia has an age and composition similar to the ash from Straning. The main part of the Pohorje Mountains igneous complex displays a clear medium to high-K calc-alkaline affinity and associated rhyodacitic dikes (Trajanova et al., 2008). The U-Pb emplacement age of the pluton is 18.64 ± 0.7 Ma and K-Ar biotite and whole rock ages range between 18.0 ± 0.7 Ma and 15.8 ± 0.7 Ma (Fodor et al., 2008; Trajanova et al., 2008). Neither rhyodacitic effusive phases, nor significant tuff horizons have been reported from the Pohorje area. The absence of abundant explosive products in the direct surroundings of the Pohorje Mountains igneous complex makes it an unlikely source for the Straning tuff. The volumetrically most significant late Burdigalian (Karpatian) acidic calc-alkaline volcanism in proximity of Straning occurred in the Inner Carpathian arc at the northern margin of the Pannonian Basin System in association with early extension and basin formation (Seghedi et al., 1998, 2004a, b, 2005; Pécskay et al., 1995, 2006; Harangi et al., 2007; Seghedi and Downes, 2011) (Fig. 11). Tuffs, tuffites and bentonite layers in Lower to Middle Miocene deposits in the Alpine-Carpathian Foredeep in the Czech Republic, Austria and Bavaria are frequently attributed to this volcanism based on its proximity, geochemistry and coincident age (Unger and Niemeyer, 1985; Unger et al., 1990; Roetzel et al., 1994, 2008; Nehyba, 1997; Adamová and Nehyba, 1998; Nehyba and Roetzel, 1999; Nehyba et al., 1999; Rocholl et al., 2008). Felsic volcanism started at about 21 Ma (early Burdigalian, Eggenburgian) in the northern Inner Carpathian volcanic arc and continued in pulses until 11 Ma (latest Serravallian, latest Sarmatian).

In the late Burdigalian (Karpatian), i.e. around 17 Ma, the production of felsic calc-alkaline rocks predominantly occurred in the area's western part (Seghedi et al., 1998; Pécskay et al., 2006). Karpatian rhyodacite tuffs and tuffites are known from the Bükk Foreland (Márton and Pécskay, 1998; Szakács et al., 1998), where two Early Miocene volcanic complexes were distinguished.

It remains difficult to compare tephras directly with volcanic source rocks, because tephra compositions are influenced by fractionation during various stages of eruption and transport, and by syn- and postdepositional processes. The geochemical composition of the Straning tephra nevertheless displays similarities with those from the Bükk Foreland (Seghedi et al., 2004a). They are e.g. similar in terms of their high K and low Mg content, their REE distribution, which displays a very similar La_N/Yb_N ratio ranging between 11.96 and 15.33 (cf. Póka

et al., 1998), and also in terms of some minor elements. Differences were recognised especially in Zr and Rb content.

The two Early Miocene volcanic horizons in the Bükk Foreland were dated to 21.5-18.5 Ma and 17.5-16.0 Ma respectively on the basis of palaeomagnetic and K/Ar results (Márton and Pécskay, 1998). The same volcanic complexes are known from the Cserhát-Mátra area in northern Hungary (Hámor et al., 1987; Zelenka et al., 2004), and the Nógrád - southern Slovakia area (Hámor et al., 1987; Vass et al., 1987) (Fig. 11).

The explosive volcanism in this western part of the Carpathian volcanic arc is the most likely source for the Straning tuff, because it corresponds in both age and composition. In particular, the middle-late Burdigalian (latest Ottnangian-earliest Karpatian) Fehérhegy Formation (formerly known as Gyulakeszi Rhyolite Tuff Formation) in northern Hungary, which is equivalent to the Middle Rhyolite Tuff complex recognized in boreholes in the Pannonian Basin, correlates well with the Straning ash (Szakács et al., 1998; Vass et al., 2006; Pálfy et al., 2007; Márton et al., 2007). This more than 80 m thick volcanoclastic series that comprises three ignimbrite horizons bearing andesitic and rhyolitic lithoclasts directly superposes the famous fossil footprints site Ipolytarnóc. The lowermost ignimbrite sheet provided an $^{40}Ar/^{39}Ar$-age of 17.02 ± 0.14 Ma (which translates into a 17.13 Ma age relative to FCs of 28.201 Ma; Kuiper et al., 2008) and a single-grain U-Pb zircon age of 17.42 ± 0.04 Ma (Pálfy et al., 2007). The uppermost of the ignimbrite sheets has a reversed polarity and likely correlates to palaeomagnetic chronozone C5Cr (Márton et al., 2007). These geochronologic and palaeomagnetic data together strongly support the age correlation with the Straning ash. It thus seems reasonable to suggest a genetic relation between the Straning ash and the Middle Rhyolite Tuff complex in northern Hungary. This would also imply westward transport of the volcanic ashes by easterly stratospheric winds at heights of about 20 km (cf. Rocholl et al., 2008).

6. Conclusions

Acidic tuffs and tuffites from the Straning outcrop at the south-eastern margin of the Bohemian Massif in Austria were dated by means of $^{40}Ar/^{39}Ar$ geochronology to 17.23 ± 0.18 Ma. They show a reversed polarity and can be correlated with the chron C5Cr of the late Burdigalian (early Karpatian) and with the lowstand systems tract (LST) of the global 3rd order sea level cycle Bur 4 of Hardenbol et al. (1998).

Geochemical results indicate that the volcanic material of the tephra beds in Straning originates from acidic (rhyodacitic to dacitic) calc-alkaline arc volcanism. A significant secondary transport/redeposition (i.e. after the fallout) and mixing with non-volcanic material is apparent. The intensity of these processes varies throughout the studied profile at Straning.

Investigations of volcanic zircon and REE reveal significant differences between the volcaniclastics from Straning and other lower and middle Burdigalian (Eggenburgian, Ottnangian) and lower Langhian (lower Badenian) tephra from the south-eastern margin of the Bohemian Massif and the Alpine-Carpathian Foredeep in Moravia and Lower Austria.

The age and geochemistry of the Straning tuffs suggest that the volcanic source was most likely located in the western Inner Carpathian volcanic arc. The Straning tuff correlates best with the Middle Rhyolite tuff (late Burdigalian, Karpatian) in Ipolytarnóc in northern Hungary.

Acknowledgements

The authors want to thank Fritz F. Steininger (Krahuletz-Museum Eggenburg) for help during fieldwork and contributing many fruitful discussions as well as initiating the palaeomagnetic study and critically reading the manuscript. We also want to thank Manfred Linner (Geological Survey Vienna) for interesting hints and for solving mineralogical problems, and Christian Rupp (Geological Survey Vienna) for information about the foraminifera. We are grateful to Helga Priewalder (Geological Survey Vienna) for the SEM- and EDS-study. We also would like to thank the Grant Agency of the Czech Republic, which kindly sponsored a part of the costs of the analytical data with the project No. 205/09/0103. Finally, we would like to thank the reviewers Franz Neubauer and Branimir Šegvić for their constructive criticism und fruitful comments.

References

Abdul Aziz, H., Böhme, M., Rocholl, A., Zwing, A., Prieto, J., Wijbrans, J.R., Heissig, K. and Bachtadse, V., 2008. Integrated stratigraphy and $^{40}Ar/^{39}Ar$ chronology of the Early to Middle Miocene Upper Freshwater Molasse in eastern Bavaria (Germany). International Journal of Earth Sciences, 97, 115-134.

Abdul Aziz, H., Böhme, M., Rocholl, A., Prieto, J., Wijbrans, J.R., Bachtadse, V. and Ulbig, A., 2010. Integrated stratigraphy and $^{40}Ar/^{39}Ar$ chronology of the early to middle Miocene Upper Freshwater Molasse in western Bavaria (Germany). International Journal of Earth Sciences, 99, 1859-1886.

Adamová, M. and Nehyba, S., 1998. Výsledky geochemického studia vulkanoklastických hornin karpatské předhlubně (Geochemistry of volcaniclastic rocks of the Carpathian Neogene foredeep). Zemný plyn a nafta, 43/2, 303-312, Hodonín (in Czech).

Balogh, K., Ebner, F., Ravasz, C., Herrmann, P., Lobitzer, H. and Solti, G., 1994. K/Ar Age of the Tertiary Volcanics of southeastern Styria and southern Burgenland (K/Ar-Alter tertiärer Vulkanite der südöstlichen Steiermark und des südlichen Burgenlands). In: H. Lobitzer, G. Császár and A. Daurer (red.), Jubiläumsschrift 20 Jahre Geologische Zusammenarbeit Österreich – Ungarn. Teil 2, pp. 55-72, Wien (Geologische Bundesanstalt) (in German).

Bedelean, I. and Mârza, I., 1991. The Volcanic Tuffs from the Transylvanian Basin, Romania. Geology – Mineralogy Department Special Issues, University of Cluj-Napoca, 464 pp.

Boynton, W.V., 1984. Cosmochemistry of the rare earth elements: meteoritic studies. In: P. Henderson (ed.), Rare Earth Elements Geochemistry. pp. 63-114, Amsterdam (Elsevier).

Bukowski, K., de Leeuw, A., Gonera, M., Kuiper, K.F., Krzywiec, P. and Peryt, D., 2010. Badenian tuffite levels within the Carpathian orogenic front (Gdów-Bochnia area, Southern Poland): Radio-isotopic dating and stratigraphic position. Geological Quarterly, 54, 449-464.

Chadima, M. and Jelínek, V., 2008. Anisoft 4.2. – Anisotropy data browser. Contribution to Geophysics and Geodesy, 38, 41.

Čižek, P., Koeppl, O., Krejčíř, M., Krmíček, P. and Pekárková, R., 1990. Lower Miocene bentonites of the Carpathian Foredeep in southern Moravia. Acta Musei Moraviae, Sci. nat., 75, 105-114, Brno.

Čtyroký, P., 1982. Spodní miocén (eggenburg a ottnang) jz. části čelní hlubiny na Moravě (The Lower Miocene (Eggenburg-Ottnang) in the SW-part of the Carpathian Foredeep in Moravia). Zemný plyn a nafta, 27, 379-394, Hodonin (in Czech).

Čtyroký, P., 1991. Členění a korelace eggenburgu a ottnangu v jižní části karpatské předhlubně na jižní Moravě (Classification and correlation of the Eggenburgian and Ottnangian in the southern part of the Carpathian Foredeep in Southern Moravia). Západné Karpaty, Séria Geológia, 15, 67-109, Bratislava (in Czech with English summary).

De Leeuw, A., Bukowski, K., Krijgsman, W. and Kuiper, K.F., 2010. Age of the Badenian salinity crisis; Impact of Miocene climate variability on the circum-mediterranean region. Geology, 38, 715-718.

De Leeuw, A., Mandic, O., Krijgsman, W., Kuiper, K. and Hrvatović, H., 2011. A chronostratigraphy for the Dinaride Lake System deposits of the Livno-Tomislavgrad Basin: the rise and fall of a long-lived lacustrine environment. Stratigraphy, 8/1, 29-43.

De Leeuw, A., Mandic, O., Krijgsman, W., Kuiper, K. and Hrvatović, H., 2012. Paleomagnetic and geochronologic constraints on the geodynamic evolution of the Central Dinarides. Tectonophysics, 530-531, 286-298.

De Leeuw, A., Filipescu, S., Maţenco, L., Krijgsman, W., Kuiper, K. and Stoica, M., 2013. Paleomagnetic and chronostratigraphic constraints on the Middle to Late Miocene evolution of the Transylvanian Basin (Romania): Implications for Central Paratethys stratigraphy and emplacement of the Tisza-Dacia plate. Global and Planetary Change, 103, 82-98.

Ebner, F., 1981. Vulkanische Tuffe im Miozän der Steiermark. Mitteilungen des naturwissenschaftlichen Vereines für Steiermark, 111 (1981), 39-55, Graz.

Ebner, F., Mali, H., Obenholzner, J.H., Vortisch, W. and Wieser, J., 1998. Pyroclastic deposits from the Middle Miocene Stallhofen Formation. Jahrbuch der Geologischen Bundesanstalt, 140/4, 425-428, Wien.

Ebner, F., Dunkl, I., Mali, H. and Sachsenhofer, R.F., 2002. Stratigraphic evidence of pyroclastic layers in Miocene basins of the Eastern Alps. Proceedings of the XVIIth Congress of the Carpathian-Balkan Geological Association, 5 p., Bratislava.

Fedo, C.M., Nesbitt, H.W. and Young, G.M., 1995. Unraveling the effects of potassium metasomatism in sedimentary rocks and paleosols, with implications for paleoweathering conditions and provenance. Geology, 23/10, 921-924.

Fisher, R.A., 1953. Dispersion on a sphere. Proceedings of the Royal Society London, 217, 295-305.

Fodor, L., Gerdes, A., Dunkl, I., Koroknai, B., Pécskay, Z., Trajanova, M., Horváth, P., Vrabec, M., Jelen, B., Balogh, K. and Frisch, W., 2008. Miocene emplacement and rapid cooling of the Pohorje pluton at the Alpine-Pannonian-Dinaridic junction, Slovenia. Swiss Journal of Geosciences, 101, Suppl. 1, S255–S271, DOI 10.1007/s00015-008-1286-9.

Füchtbauer, H., 1959. Zur Nomenklatur der Sedimentgesteine. Erdöl und Kohle, 12/8, 605-613.

Gradstein, F.M., Ogg, J.G., Schmitz, M.D. and Ogg, G.M., 2012. The geological time scale 2012. Vol. 2, x + pp. 437-1144, Elsevier.

Grunert, P., Soliman, A., Harzhauser, M., Müllegger, S., Piller, W., Roetzel, R. and Rögl, F., 2010. Upwelling conditions in the Early Miocene Central Paratethys Sea. Geologica Carpathica, 61/2, 129-145.

Hámor, G., Ravasz-Baranyai, L., Halmai, J., Balogh, K. and Árva-Sós, E., 1987. Dating of Miocene acid and intermediate volcanic activity in Hungary. Proceedings of the 8th RCMNS Congress, Annals of the Hungarian Geological Institute, 70, 149-154, Budapest.

Handler, R., Ebner, F., Neubauer, F., Bojar, A.V. and Hermann, S., 2006. $^{40}Ar/^{39}Ar$ dating of Miocene tuffs from the Styrian part of the Pannonian Basin: An attempt to refine the basin stratigraphy. Geologica Carpathica, 57/6, 483-494.

Harangi, S., Downes, H. and Seghedi, I., 2006. Tertiary-Quaternary subduction processes and related magmatism in the Alpine-Mediterranean region. In: D.G. Gee and R.A. Stephenson (eds.), European Lithosphere Dynamics. Geological Society of London, Memoirs, 32, 167-190.

Harangi, S., Downes, H., Thirlwall, M. and Gméling, K., 2007. Geochemistry, Petrogenesis and Geodynamic Relationships of Miocene Calc-alkaline Volcanic Rocks in the Western Carpathian Arc, Eastern Central Europe. Journal of Petrology, 48/12, 2261-2287.

Hardenbol, J., Thierry, J., Farley, M.B., Jacquin, T., de Graciansky, P.C. and Vail, P.R., 1998. Mesozoic and Cenozoic sequence chronostratigraphic framework of European Basins. In: P.C. de Graciansky, J. Hardenbol, T. Jacquin and P.R. Vail (eds.), Mesozoic and Cenozoic sequence stratigraphy of European Basins. SEPM Special Publication, 60, pp. 3-13.

Hölzel, M. and Wagreich, M., 2004. Sedimentology of a Miocene delta complex: The type section of the Ingering Formation (Fohnsdorf Basin, Austria). Austrian Journal of Earth Sciences, 95/96, 80-86.

Hüsing, S.K., Kuiper, K.F., Link, W., Hilgen, F.J. and Krijgsman, W., 2009. The upper Tortonian–lower Messinian at Monte dei Corvi (Northern Apennines, Italy): Completing a Mediterranean reference section for the Tortonian Stage. Earth and Planetary Science Letters, 282/1-4, 140-157.

Irvine, T.N. and Baragar, W.R.A., 1971. A guide to the chemical classification of the common volcanic rocks. Canadian Journal of Earth Sciences, 8/5, 523-548.

Jurková, A. and Tomšík, J., 1959. Tufitické horniny v tortonu ostravsko-karvinského revíru (Tuffites within the Tortonian of the Ostrava-Karvina coal district). Časopis pro mineralogii a geologii, 4/4, 394-407, Praha (in Czech).

Kempf, O. and Pross, J., 2005. The lower marine to lower freshwater Molasse transition in the northern Alpine foreland basin (Oligocene; central Switzerland – south Germany): age and geodynamic implications. International Journal of Earth Sciences, 94/1, 160-171.

Kirschvink, J.L., 1980. The least-squares line and plane and the analysis of paleomagnetic data. Geophysical Journal of the Royal Astronomical Society, 62, 699-718.

Koppers, A.A.P., 2002. ArArCALC-software for $^{40}Ar/^{39}Ar$ age calculations. Computers and Geosciences, 28, 605–619.

Kowallis, B.J., Christiansen, E.H. and Deino, A., 1989. Multicharacteristic correlation of Upper Cretaceous volcanic ash beds from southwestern Utah to Central Colorado. Utah Geological and Mineral Survey, Miscellaneous Publication, 89/5, 1-12.

Kowallis, B.J. and Christiansen, E.H., 1990. Applications of zircon morphology: correlation of pyroclastic rocks and petrogenetic differences. Abstracts of field conference and workshop on tephrochronology, Mammoth Hot Springs, June 1990, 25, Wyoming.

Krijgsman, W., Hilgen, F.J., Negri, A., Wijbrans, J.R. and Zachariasse, W.J., 1997. The Monte del Casino section (Northern Apennines, Italy): a potential Tortonian/Messinian boundary stratotype?. Palaeogeography, Palaeoclimatology, Palaeoecology, 133/1–2, 27-47.

Krystek, I., 1959. Petrografie tufitických hornin z oblasti vídeňské vnitrokarpatské a vněkarpatské pánve (Petrography of tuffitic rocks in the Vienna, Inner and Outer Carpathian Basin). Geologické práce, 54, 127-144, Bratislava (in Slovak with German summary).

Krystek, I., 1983. Výsledky faciálního a paleogeografického výzkumu mladšího terciéru na jv. svazích Českého masivu v úseku "Jih" (Results of facial and paleogeographical study of younger Tertiary on SE slopes of Bohemian Massif in the section „South"). Folia Facultatis Scientiarum Naturalium Universitatis Purkynianae Brunensis. Geologia, 24/9, 1-47, Brno (in Czech).

Kuiper, K.F., Deino, A., Hilgen, F.J., Krijgsman, W., Renne, P.R. and Wijbrans, J.R., 2008. Synchronizing rock clocks of Earth history. Science, 320, 500.

Leat, P.T., Jackson, S.E., Thorpe, R.S. and Stillman, C.J., 1986. Geochemistry of bimodal basalt-subalkaline/peralkaline rhyolite provinces within the Southern British Caledonides. Journal of the Geolological Society, London, 143, 259-273.

Le Maitre, R.W., 1984. A proposal by the IUGS subcommission on the systematics of igneous rocks for chemical classification of volcanic rocks based on the total alkali silica (TAS) diagram. Australian Journal of Earth Sciences, 31, 243-255.

Le Maitre, R.W. (ed.), Bateman, P., Dudek, A., Keller, J., Lameyre, M., Le Bas, M.J., Sabine, P.A., Schmid, R., Sørensen, H., Streckeisen, A., Wolley, A.R. and Zanettin, B., 1989. A classification of igneous rocks and a glossary of terms. Recommendations of the International Union of Geological Sciences Subcommission on the Systematics of Igneous Rocks. 193 pp., Oxford (Blackwell).

Lustrino, M. and Wilson, M., 2007. The circum-Mediterranean anorogenic Cenozoic igneous province. Earth-Science Reviews, 81, 1-65.

Mandic, O., de Leeuw, A., Vukoviç, B., Krijgsman, W., Harzhauser, M. and Kuiper, K.F., 2011. Palaeoenvironmental evolution of Lake Gacko (NE Bosnia and Herzegovina): impact of the Middle Miocene Climatic Optimum on the Dinaride Lake System. Palaeogeography, Palaeoclimatology, Palaeoecology, 299/3-4, 475-492.

Mandic, O., de Leeuw, A., Bulić, J., Kuiper, K., Krijgsman, W. and Jurišić-Polšak, Z., 2012. Paleogeographic evolution of the Southern Pannonian Basin: $^{40}Ar/^{39}Ar$ age constraints on the Miocene continental series of Northern Croatia. International Journal of Earth Sciences, 101, 1033-1046.

Márton, E. and Pécskay, Z., 1998. Correlation and dating of the Miocene ignimbritic volcanics in the Bükk Foreland, Hungary: complex evaluation of paleomagnetic and K/Ar isotope data. Acta Geologica Hungarica, 41, 467-476.

Márton, E., Vass, D., Túnyi, I., Márton, P. and Zelenka, T., 2007. Paleomagnetic properties of the ignimbrites from the famous fossil footprints site, Ipolytarnóc (close to the Hungarian-Slovak frontier) and their age assignment. Geologica Carpathica, 58/6, 531-540.

McFadden, P.L. and McElhinny, M.W., 1990. Classification of the reversal test in palaeomagnetism. Geophysical Journal International, 103, 725-729.

Montanari, A., Carey, S., Coccioni, R. and Deino, A., 1994. Early Miocene tephra in the Apennine pelagic sequence: An inferred Sardinian provenance and implications for western Mediterranean tectonics. Tectonics, 13/5, 1120-1134.

Moore, D. M. and Reynolds, Jr. R.C., 1997. X-Ray Diffraction and the Identification and Analysis of Clay Minerals. 378 pp., New York (Oxford Univ. Press).

Müller, G., 1961. Das Sand-Silt-Ton-Verhältnis in rezenten marinen Sedimenten. Neues Jahrbuch für Mineralogie, Monatshefte, 1961, 148-163.

Nehyba, S., 1997. Miocene volcaniclastics of the Carpathian Foredeep in the Czech Republic. Věstník Českého geologického ústavu, 72/4, 311-327, Praha.

Nehyba, S. and Roetzel, R., 1999. Lower Miocene volcaniclastics in South Moravia and Lower Austria. Jahrbuch der Geologischen Bundesanstalt, 141/4, 473-490, Wien.

Nehyba, S., Roetzel, R. and Adamová, M., 1999. Tephrostratigraphy of the Neogene volcaniclastics (Moravia, Lower Austria, Poland). Geologica Carpathica, 50, Special Issue, 126-128.

Nehyba, S., 2000. Middle Badenian volcaniclastics in the drill hole OS-2 Hať near Hlučín (Silezia). Geologické výzkumy na Moravě a ve Slezsku v roce 1999, 69-72, Brno (in Czech).

Nehyba, S. and Stráník, Z., 2005. Volcaniclastics within the Pavlovice Formation of the Ždanice Unit. Geologické výzkumy na Moravě a ve Slezsku v roce 2004, 12/1, 37-41, Brno (in Czech).

Nesbitt, H.W. and Young, G.M., 1982. Early Proterozoic climates and plate motions inferred from major element chemistry of lutites. Nature, 299/21, 715–717.

Pálfy, J., Mundil, R., Renne, P.R., Bernor, R.L., Kordos, L. and Gasparik, M., 2007. U-Pb and $^{40}Ar/^{39}Ar$ dating of the Miocene fossil track site at Ipolytarnóc (Hungary) and its implications. Earth and Planetary Science Letters, 258, 160-174.

Pearce, J.A., Harris, N.B.W. and Tindle, A.G., 1984. Trace element discrimination diagrams for the tectonic interpretation of granitic rocks. Journal of Petrology, 25, 956-983.

Pécskay, Z., Lexa, J., Szakács, A., Balogh, K., Seghedi, I., Konečny, V., Kovács, M., Márton, E., Kaličiak, M., Széky-Fux, V., Póka, T., Gyarmati, P., Edelstein, O., Roşu, E. and Žec, B., 1995. Space and time distribution of Neogene-Quaternary volcanism in the Carpatho-Pannonian Region. Acta Vulcanologica, Special Issue, 7/2, 15-28.

Pécskay, Z., Lexa, J., Szakács, A., Seghedi, I., Balogh, K., Konečný, V., Zelenka, T., Kovacs, M., Póka, T., Fülöp, A., Márton, E., Panaiotu, C. and Cvetkovic, V., 2006. Geochronology of Neogene magmatism in the Carpathian arc and intra-Carpathian area. Geologica Carpathica, 57, 511-530.

Piller, W.E., Harzhauser, M. and Mandic, O., 2007. Miocene Central Paratethys stratigraphy – current status and future directions. Stratigraphy, 4/2-3, 151-168.

Póka, T., Zelenka, T., Szakács, A., Seghedi, I., Nagy, G. and Simonits, A., 1998. Petrology and geochemistry of the Miocene acidic explosive volcanism of the Bükk Foreland, Pannonian Basin, Hungary. Acta Geologica Hungarica, 41/4, 437-466.

Pouchou, J.L. and Pichoir, F., 1985. "PAP" (φ-ρ-Z) procedure for improved quantitative microanalysis. In: J.T. Armstrong (ed.), Microbeam Analysis, 104–106, San Francisco Press.

Poultidis, H. and Scharbert, H.G., 1987. Bericht über geochemisch-petrologische Untersuchungen an basaltischen Gesteinen des österreichischen Teils der transdanubischen vulkanischen Region. Anzeiger der Österreichischen Akademie der Wissenschaften, math.-naturwiss. Klasse, 123 (1986), 65-76, Wien.

Pupin, J.P., 1980. Zircon and Granite Petrology. Contributions to Mineralogy and Petrology, 73, 207-220.

Pupin, J.P., 1985. Magmatic zoning of hercynian granitoids in France based on zircon typology. Schweizer mineralogische und petrographische Mitteilungen, 65, 29-56.

Pūspōki, Z., Kozák, M., Kovács-Pálffy, P., Fōldvári, M., McIntosh, R.W. and Vincze, L., 2005. Eustatic and Tectonic/Volcanic Control in Sedimentary Bentonite Formation - A Case Study of Miocene Bentonite Deposits from the Pannonian Basin. Clays and Clay Minerals, 53/1, 71-91, 10.1346/ccmn.2005.0530108.

Raschka, H., 1912. Die Rutschungen in dem Abschnitte Ziersdorf - Eggenburg der Kaiser Franz Josef-Bahn (Hauptstrecke). Zeitschrift des Österr. Ingenieur- u. Architekten-Vereins, 64/36, 561-566, Wien.

Reischmann, T. and Schraft, A., 2009. Der Vogelsberg – Geotope im größten Vulkangebiet Mitteleuropas. 252 pp., Wiesbaden (Hessisches Landesamt für Umwelt und Geologie).

Reitner, H., Malecki, G. and Roetzel, R., 2005. SedPacWin – SedpacMac - Characterization of Sediments by Grainsize Analysis. Geophysical Research Abstracts, 7, EGU General Assembly Vienna, 24.-29. April 2005, SRef-ID: 1607-7962/gra/EGU05-A-04297, Wien.

Rocholl, A., Boehme, M., Guenther, D., Höfer, H. and Ulbig, A., 2008. Prevailing stratospheric easterly wind direction in the Paratethys during the Lower Badenian: Ar-Ar- and Nd-isotopic evidence from rhyolitic ash layers in the Upper Freshwater Molasse, S-Germany. Geophysical Research Abstracts, 10, EGU General Assembly Vienna, 13.-18. April 2008, SRef-ID: 1607-7962/gra/EGU2008-A-08747, Wien.

Roetzel, R., 1994. Bericht 1993 über geologische Aufnahmen im Tertiär und Quartär im Raum Grafenberg-Maissau auf Blatt 22 Hollabrunn. Jahrbuch der Geologischen Bundesanstalt, 137/3, 435-438, Wien.

Roetzel, R., Ottner, F., Schwaighofer, B. and Müller, H.W., 1994. Tertiäre Tone am Ostrand der Böhmischen Masse. In: E.E. Kohler (ed.), Berichte der dt. Ton- und Tonmineralgruppe e.V.. Beiträge zur Jahrestagung Regensburg, 13.-14. Okt. 1994, pp. 111-122, Regensburg.

Roetzel, R., 1996. Bericht 1994/1995 über geologische Aufnahmen im Tertiär und Quartär mit Bemerkungen zur Tektonik am Diendorfer Störungssystem auf Blatt 22 Hollabrunn. Jahrbuch der Geologischen Bundesanstalt, 139/3, 286-295, Wien.

Roetzel, R. [Bearbeitung], Batík, P., Cicha, I., Havlíček, P., Holásek, O., Novák, Z., Pálenský, P., Roetzel, R., Rudolský, J., Růžička, M., Stráník, Z., Švábenická, L., Vůjta, M., Hofmann, Th. and Hellerschmidt-Alber, J., 1998. Geologische Karte der Republik Österreich 1:50.000 22 Hollabrunn, Wien (Geologische Bundesanstalt).

Roetzel, R., Mandic, O. and Steininger, F. F., 1999a. Lithostratigraphie und Chronostratigraphie der tertiären Sedimente im westlichen Weinviertel und angrenzenden Waldviertel. In: R. Roetzel (ed.), Arbeitstagung der Geologischen Bundesanstalt 1999 - Retz-Hollabrunn. pp. 38-54, Wien (Geologische Bundesanstalt).

Roetzel, R., Scharbert, S., Wimmer-Frey, I. and Decker, K., 1999b. B3 Straning – Bahneinschnitt. In: R. Roetzel (ed.), Arbeitstagung der Geologischen Bundesanstalt 1999 - Retz-Hollabrunn. pp. 290-293, Wien (Geologische Bundesanstalt).

Roetzel, R., Řeháková, Z., Cicha, I., Decker, K. and Wimmer-Frey, I., 1999c. B6 Parisdorf - Diatomitbergbau Wienerberger. In: R. Roetzel (ed.), Arbeitstagung der Geologischen Bundesanstalt 1999 - Retz-Hollabrunn. pp. 306-311, Wien (Geologische Bundesanstalt).

Roetzel, R., Ćorić, S., Galović, I. and Rögl, F., 2006. Early Miocene (Ottnangian) coastal upwelling conditions along the southeastern scarp of the Bohemian Massif (Parisdorf, Lower Austria, Central Paratethys). Beiträge Paläontologie, 30, 387-413, Wien.

Roetzel, R., Fuchs, G., Ahl, A., Schubert, G. and Slapansky, P., 2008. Erläuterungen zu Blatt 8 Geras. 136 pp., Wien (Geologische Bundesanstalt).

Roštínský, P. and Roetzel, R., 2005. Exhumed Cenozoic landforms on the SE flank of the Bohemian Massif in the Czech Republic and Austria. Zeitschrift für Geomorphologie, N.F., 49/1, 23-45.

Roy, P.D., Caballero, M., Lozano, R. and Smykatz-Kloss W., 2008. Geochemistry of late quaternary sediments from Tecocomulco lake, central Mexico: Implication to chemical weathering and provenance. Chemie der Erde, 68, 383-393.

Schaffer, F. X. and Grill, R., 1951. Die Molassezone. In: F.X. Schaffer (ed.), Geologie von Österreich. 2.Aufl., pp. 694-761, Wien (Deuticke).

Schubert, G., Safoschnik, T., Supper, R., Bernhard, M., Felfer, W. and Roetzel, R., 1999. B1 Das Becken von Obermarkersdorf. In: R. Roetzel (ed.), Arbeitstagung der Geologischen Bundesanstalt 1999 - Retz-Hollabrunn. pp. 279-286, Wien (Geologische Bundesanstalt).

Schultz, L. G., 1964. Quantitative Interpretation of Mineralogical Composition from X-ray and Chemical data for the Pierre Shale. Geological Survey Professional Paper 391-C, pp. C1-C31, United States Government Printing Office, Washington.

Seghedi, I., Balintoni, I. and Szakács, A., 1998. Interplay of tectonics and neogene post-collisional magmatism in the intracarpathian region. Lithos, 45, 483–497.

Seghedi, I., Downes, H., Szakács, A., Mason, P. R. D., Thirlwall, M.F., Roşu, E., Pécskay, Z., Márton, E. and Panaiotu, C., 2004a. Neogene-Quaternary magmatism and geodynamics in the Carpathian-Pannonian region: a synthesis. Lithos, 72, 117-146.

Seghedi, I., Downes, H., Vaselli, O., Szakács, A., Balogh, K. and Pécskay, Z., 2004b. Post-collisional Tertiary–Quaternary mafic alkali magmatism in the Carpathian–Pannonian region: a review. Tectonophysics, 393/1-4, 43-62.

Seghedi, I., Downes, H., Harangi, S., Mason, P.R.D. and Pécskay, Z., 2005. Geochemical response of magmas to Neogene–Quaternary continental collision in the Carpathian–Pannonian region: a review. Tectonophysics, 410, 485-499.

Seghedi, I. and Downes, H., 2011. Geochemistry and tectonic development of Cenozoic magmatism in the Carpathian-Pannonian region. Gondwana Research, 20/4, 655-672.

Šegvić, B., Mileusnić, M., Aljinović, D., Vranjković, A., Mandic, O., Pavelić, D., Dragičević, I. and Ferreiro Mählmann, R., 2014. The Provenance and Diagenesis of Tuffs from the Dinaride Lake System (Miocene, Southern Croatia). European Journal of Mineralogy, 26, 83-101, DOI: 10.1127/0935-1221/2013/0025-2350.

Steiger, R.H. and Jäger, E., 1977. Subcommission on geochronology: convention on the use of decay constants in geo- and cosmochronology. Earth and Planetary Science Letters, 36, 359-362.

Steininger, F.F. and Bagdasarjan, G.P., 1977. Neue radiometrische Alter mittelmiozäner Vulkanite der Steiermark (Österreich), ihre biostratigraphische Korrelation und ihre mögliche Stellung innerhalb der paläomagnetischen Zeitskala. Verhandlungen der Geologischen Bundesanstalt, 1977/2, 85-99, Wien.

Steininger, F.F., Daxner-Höck, G., Haas, M., Kovar-Eder, J., Mauritsch, H., Meller, B. and Scholger, R.M., 1998. Stratigraphy of the "Basin Fill" in the Early Miocene Lignite Opencast Mine Oberdorf (N Voitsberg, Styria, Austria). Jahrbuch der Geologischen Bundesanstalt, 140/4, 491-496, Wien.

Strauss, P.E., Daxner-Höck, G. and Wagreich, M., 2003. Lithostratigraphie, Biostratigraphie und Sedimentologie des Miozäns im Fohnsdorfer Becken (Österreich). Stratigraphia Austriaca, Österreichische Akademie der Wissenschaften, Schriftenreihe der Erdwissenschaftlichen Kommissionen, 16, 111-140, Wien.

Szakács, A., Zelenka, T., Márton, E., Pécskay, Z., Póka, T. and Seghedi, I., 1998. Miocene acidic explosive volcanism in the Bükk Foreland, Hungary: Identifying eruptive sequences and searching for source locations. Acta Geologica Hungarica, 41/4, 413-43.

Szakács, A., Pécskay, Z., Lóránd, S., Balogh, K., Vlad, D. and Fülöp, A., 2012. On the age of the Dej Tuff, Transylvanian Basin (Romania). Geologica Carpathica, 63/2, 139-148.

Trajanova, M. and Pécskay, Z., 2006. Evolution of the calc-alkaline magmatism in the Pohorje Mt., Slovenia. In: M. Sudar, M. Ercegovac and A. Grubic (eds.), Proceedings of the XVIIIth Congress of the Carpathian-Balkan Geological Association. pp. 632-635, Belgrade.

Trajanova, M., Pécskay, Z. and Itaya, T., 2008. K-Ar geochronology and petrography of the Miocene Pohorje Mountains batholith (Slovenia). Geologica Carpathica, 59/3, 247-260.

Unger, H.J. and Niemeyer, A., 1985. Die Bentonite in Ostniederbayern – Entstehung, Lagerung, Verbreitung. Geologisches Jahrbuch, D71, 3-58.

Unger, H.J., Fiest, W. and Niemeyer, A., 1990. Die Bentonite der ostbayerischen Molasse und ihre Beziehungen zu den Vulkaniten des Pannonischen Beckens. Geologisches Jahrbuch, D96, 67-112.

Vass, D., Elečko, M., Kantorová, V., Lehotayová, R. and Klubert, J., 1987. Prvý nález morského otnangu v juhoslovenskej panve (The first discovery of marine Ottnangian in the South Slovakian Basin). Mineralia Slovaca, 19/5, 417-422, Bratislava (in Slovak with English summary).

Vass, D., Túnyi, I. and Márton, E., 2006. The Fehér hegy Formation: Felsitic ignimbrites and tuffs at Ipolytarnóc (Hungary), their age and position in Lower Miocene of Northern Hungary and Southern Slovakia. Slovak Geological Magazine, 12/2, 139-145.

Wieser, T., 1985. The teschenite formation and other evidences of magmatic activity in the Polish Flysch Carpathians and their geotectonic and stratigraphic significance. In: T. Wieser (ed.), Fundamental research in the Western part of the Polish Carpathians. pp. 23-36, Cracow.

Wijbrans, J., Németh, K., Martin, U. and Balogh, K., 2007. $^{40}Ar/^{39}Ar$ geochronology of Neogene phreatomagmatic volcanism in the western Pannonian Basin, Hungary. Journal of Volcanology and Geothermal Research, 164, 193-204.

Wilson, M. and Downes, H., 1992. Mafic alkaline magmatism associated with the European Cenozoic rift system. In: P.A. Ziegler (ed.), Geodynamics of Rifting, Volume I. Case History Studies on Rifts: Europe and Asia. Tectonophysics, 208, pp. 173-182.

Winchester, J.A. and Floyd, P.A., 1977. Geochemical discrimination of different magma series and their differentiation products using immobile elements. Chemical Geology, 20, 325-343.

Zelenka, T., Balázs, E., Balogh, K., Kiss, J., Kozák, M., Nemesi, L., Pécskay, Z., Püspőki, Z., Ravasz, Cs., Széky-Fux, V. and Ujfalussy, A., 2004. Buried Neogene volcanic structures in Hungary. Acta Geologica Hungarica, 47/2-3, 177-219.

Zijderveld, J.D.A., 1967. A.C. demagnetization of rocks. In: D. W. Collinson, K.M. Creer and S.K. Runcorn (eds.), Methods in paleomagnetism. pp. 245-286, Amsterdam (Elsevier).

Zimmerle, W., 1979. Accessory Zircon from a Rhyolite, Yellowstone National Park (Wyoming, U.S.A.). Zeitschrift der Deutschen Geologischen Gesellschaft, 130, 361-369, Hannover.

Received: 12 December 2013
Accepted: 19 May 2014

Reinhard ROETZEL[1)*], Arjan de LEEUW[2)], Oleg MANDIC[3)], Emő MÁRTON[4)], Slavomír NEHYBA[5)], Klaudia F. KUIPER[6)], Robert SCHOLGER[7)] & Ingeborg WIMMER-FREY[1)]

[1)] Geological Survey, Neulinggasse 38, 1030 Wien, Austria;

[2)] CASP, West Building, 181A Huntingdon Road, Cambridge, CB3 0DH, United Kingdom;

[3)] Department of Geology and Palaeontology, Natural History Museum Vienna, Burgring 7, 1014 Wien, Austria;

[4)] Palaeomagnetic Laboratory, Geological and Geophysical Institute of Hungary, Columbus 17-23, 1145 Budapest, Hungary;

[5)] Institute of Geological Sciences, Faculty of Science, Masaryk University, Kotlářská 2, 611 37 Brno, Czech Republic;

[6)] Faculty of Earth and Life Sciences, Vrije Universiteit Amsterdam, De Boelelaan 1085, 1081 HV Amsterdam, The Netherlands;

[7)] Department of Applied Geological Sciences and Geophysics, University of Leoben, Peter-Tunner-Straße 25, 8700 Leoben, Austria;

[*)] Corresponding author, reinhard.roetzel@geologie.ac.at